Geomorphology 295 (2017) 215–234

Contents lists available at ScienceDirect

Geomorphology

journal homepage: www.elsevier.com/locate/geomorph

Natural levee evolution in the Rhine-Meuse delta, the Netherlands, during the first millennium CE

H.J. Pierik[a,*], E. Stouthamer[a], K.M. Cohen[a,b,c]

[a] Department of Physical Geography, Faculty of Geosciences, Utrecht University, PO Box 80.115, 3508 TC Utrecht, The Netherlands
[b] Deltares, Dept. Applied Geology and Geophysics, PO Box 85.467, 3508 AL Utrecht, The Netherlands
[c] TNO Geological Survey of the Netherlands, PO Box 80.015, 3508 TA Utrecht, The Netherlands

ARTICLE INFO

Keywords:
Natural levee
Delta topography
Fluvial geomorphology
Rhine-Meuse delta

ABSTRACT

This paper presents reconstructions on natural levee development in the Rhine-Meuse delta, the Netherlands, during the first millennium CE, covering the full delta plain. It is the first study that performs this on a delta scale, which allows seeing the delta-wide trends on levee-forming controls and their feedbacks. We mapped the levee morphology and elevation by combining LiDAR imagery, lithological borehole data, soil mapping, radiocarbon dates, archaeological data, and GIS-reconstruction techniques. From the detailed levee reconstructions we quantified natural levee dimensions and evaluated the temporal changes therein. The dimensions and the changes therein were then linked to external forcings (increasing suspended sediment load, variable flooding intensity) and to natural preconditions (e.g., delta plain width, flood basin configuration).

We show that natural preconditions are an important control on levee shape. This is demonstrated for the upper delta where the relatively narrow delta plain combined with strong compartmentation (i.e., the occurrence of many alluvial ridges and enclosed flood basins) caused the flood levels to be amplified allowing the natural levees to grow relatively high. Compartmentation also seems to have stimulated trapping of coarse-grained overbank sediments, explaining the clear downstream trend in levee width. This effect was probably further aided by the clearance of the riparian forests, mainly in the upstream and central delta, which caused the coarser fraction of the suspended load to be further dispersed into the flood basin leading to wider levees. In the first millennium CE several new river courses formed that avoided the areas of natural levee relief of abandoned alluvial ridges. On these fossil alluvial ridges, the topographical expression gradually reduced because of widespread flood basin trapping of overbank sediment, which led to topographic levelling. The natural levees that formed during this period along the new courses appear to be relatively high compared to precursor generations in the upper and central delta. This is most likely related to the increased suspended sediment supply and intense flooding regime during their formation. The hypotheses generated with this new delta-wide overview help to better understand the controls in the development of levees, which are important elements in river landscapes and in fluvial sedimentary records.

1. Introduction

Natural levees are pronounced geomorphological features in the low-relief floodplain topography of river and delta landscapes (e.g., Fisk, 1947; Allen, 1965). Because of their relief expression, natural levees affect floodplain hydraulics and overbank sedimentation. As such, they are also key elements in the formation of channels and fluvial sedimentary records (e.g., Brierley et al., 1997; Törnqvist and Bridge, 2002; Filgueira-Rivera et al., 2007). As natural levees are the main areas of human occupation in wet delta landscapes, they are also important for understanding the interaction between the active delta landscape and coeval human occupation (e.g., Modderman, 1948; Hudson, 2004; Guccione, 2008; Funabiki et al., 2012; Pierik and Van Lanen, 2017; Van Dinter et al., 2017). The size, shape, and height of natural levees strongly varies between rivers and within deltas, owing to differences in sediment supply, duration of sedimentation, and flood regime (Hudson and Heitmuller, 2003; Adams et al., 2004). Their formative controls have typically been analysed as case studies for specific selected meander bends, mainly for active sedimentary environments (e.g., Cazanacli and Smith, 1998; Törnqvist and Bridge, 2002; Hudson and Heitmuller, 2003; Filgueira-Rivera et al., 2007; Smith and Perez-Arlucea, 2008; Smith et al., 2009; Heitmuller et al., 2017). These

* Corresponding author.
E-mail address: h.j.pierik@uu.nl (H.J. Pierik).

http://dx.doi.org/10.1016/j.geomorph.2017.07.003
Received 2 February 2017; Received in revised form 3 July 2017; Accepted 3 July 2017
Available online 05 July 2017
0169-555X/

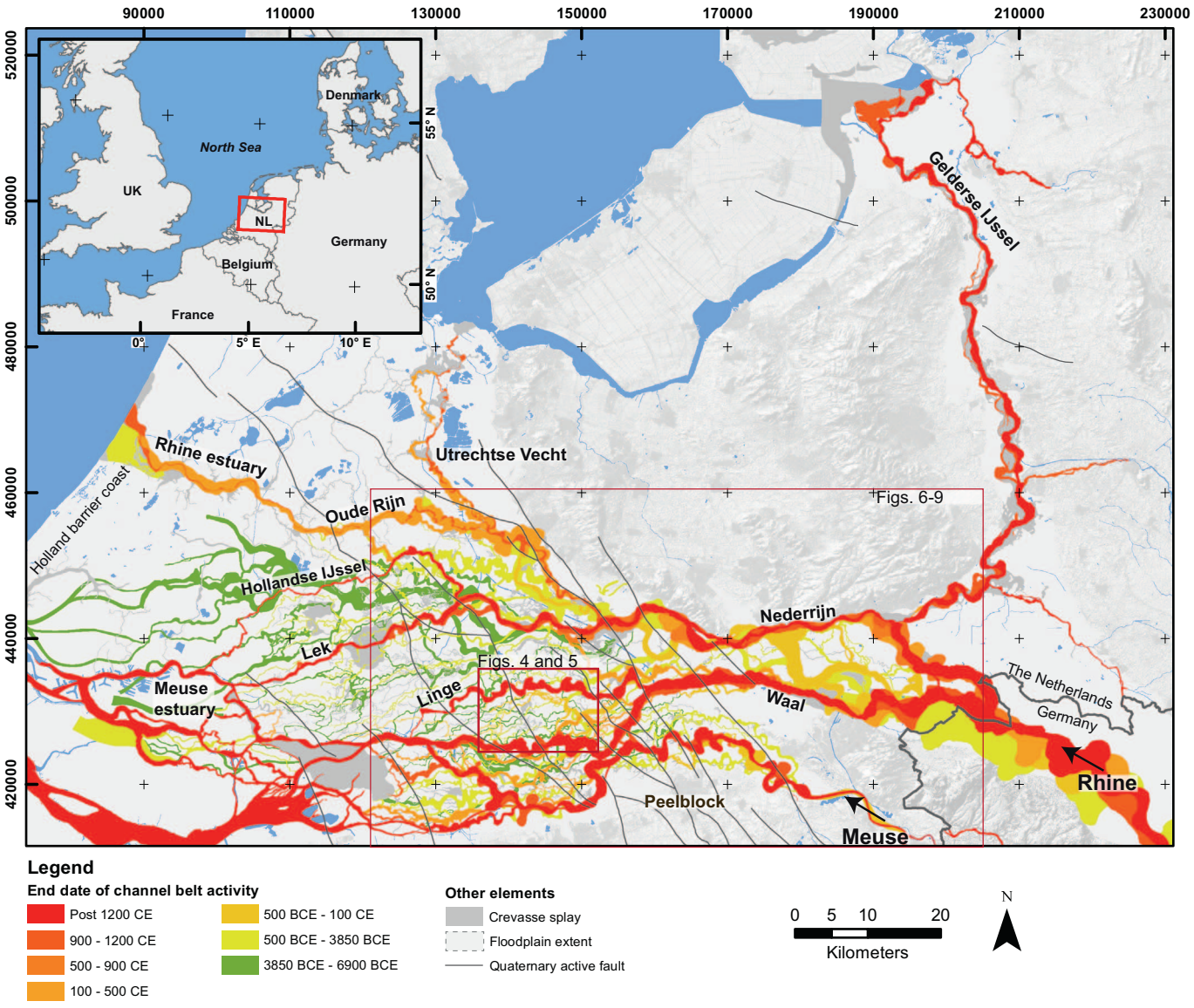

Fig. 1. Location of the study area within the Rhine-Meuse delta. Network of channel belts after Berendsen and Stouthamer (2000) and Cohen et al. (2012).

studies mainly provide insight into short-term sedimentary processes involved in local levee formation. The diverse morphology of levees, however, also is a product of regional variation in natural preconditions — the geomorphological setting of the delta and the flood basins (e.g., Kleinhans et al., 2013; Klasz et al., 2014; Lewin and Ashworth, 2014; Van Asselen et al., 2017) — that is often missed in local case studies. The regional variation in the natural preconditions includes differences in delta plain width, flood basin configuration, substrate, and the prior avulsion history. These conditions affect typical flood height that in turn controls levee height and shape and makes overbank sedimentation vary within the delta, along channels, and through successive stages. This setting needs to be studied on a regional scale before dimensions of individual levees can be well understood. A delta-wide analysis therefore is necessary to study the variation in dimensions of natural levees and their formative controls in space and time.

In this paper we map the natural levees of the Rhine-Meuse delta in the Netherlands (Fig. 1) and interpret the inferred patterns as the outcome of the inherited setting, external forcings, and internal geomorphic process factors. This is a suitable area to conduct such a study because of data abundance: LiDAR surface data sets, dense subsurface data from borehole databases, and well-developed age control on landscape development (e.g., Berendsen and Stouthamer, 2000; Gouw, 2008; Cohen et al., 2012). Natural levees in this delta (as in other deltas) have been studied before, but mostly as local case studies only. Natural levees show up as elements in individual detailed local mapping projects that seldom cover areas > 50 km^2. Levee extent and thickness have also been investigated using detailed local cross sections (e.g., Törnqvist and Bridge, 2002), delta-wide cross sections (e.g., Gouw and Erkens, 2007), and regional geomorphological and geoarchaeological mapping (e.g., Berendsen, 1982; Willems, 1986; Van Dinter, 2013). When comparing these studies, which each have slightly different methods and definitions when distinguishing the levees, the large diversity in levee width, elevation, and distribution across the Rhine-Meuse delta becomes evident. A uniform mapping and synthesis of the levee characteristics across the Rhine-Meuse delta so far has not been attempted, and the factors that explain levee shape variability have remained unexplored on the delta scale.

In the next sections, we (i) determine and quantify the changes in natural levee patterns, shape, distribution, and elevation in the Rhine-Meuse delta throughout the first millennium CE and (ii) use these results to assess the role of varying forcings, natural preconditions, and feedbacks in the development of natural levees in this area. The levee geomorphology was mapped for consecutive time slices in the first millennium CE (100, 500, and 900 CE) because the landscape from this

period has been well preserved and is best resolved using LiDAR and borehole data. The large-scale construction of dikes from ca. 1050 CE onward caused sedimentation to be restricted to the narrow corridors of the embanked floodplain (Hesselink et al., 2003; Hudson et al., 2008). This caused the fossil levee landscape in the rest of the delta plain to remain at a rather shallow depth below the current surface, which enhanced the possibilities for mapping the levees.

The natural preconditions in the beginning of the first millennium CE (e.g., the width of the delta plain and the substrate composition) vary greatly between the upper and central regions of the delta. Over the studied period, major geomorphological changes occurred to which the levees presumably adjusted. For example, a series of avulsions redistributed discharge of Rhine water and sediment over the delta (Stouthamer and Berendsen, 2001), suspended sediment load was higher than in previous periods (Erkens et al., 2011), and the frequency of large floods increased (Toonen et al., 2013). These independently reconstructed, varying natural preconditions and external forcings were compared to natural levee shape and the developments therein observed in the levee reconstructions. The time steps of the reconstructions (100, 500, and 900 CE) equally divide the first millennium and the phasing of the avulsions and changing forcings. By comparing the differences in levee shape across the entire delta throughout the first millennium CE, the regional controls on levee formation are inferred. This leads to a more complete identification of the processes and controls involved in levee formation.

2. The Rhine-Meuse delta: setting and natural levee characteristics

2.1. Delta evolution

The Rhine-Meuse delta extends from its apex in the Dutch-German border region westward to the Holland barrier coast (Fig. 1). Near the delta apex, the Rhine floodplain is up to 20 km wide; but in the downstream direction it first narrows to ca. 10 km (near X = 190,000; Fig. 1) before widening again to 50 km in the central and lower parts of the delta. The thickness of the Holocene deposits increases from a few meters in the upper delta to about 20 m near the coastline. This deltaic wedge contains flood basin clays and peat intersected by sand bodies of multiple generations of channel belts topped and flanked by levee complexes (e.g., Törnqvist, 1993; Weerts, 1996; Gouw and Erkens, 2007; Makaske et al., 2007). In the upstream delta, wide alluvial ridges enclose relatively small flood basins; whereas westward, increasingly confined alluvial ridges separate much larger flood basins (Törnqvist, 1993; Makaske et al., 2007; Gouw, 2008). In the upstream part the overbank material is more silty, and the presence of vegetation horizons indicates mainly nonpermanent inundation of the flood basins (Egberts, 1950; Havinga, 1969); whereas in the downstream part, peat indicates semipermanent and permanent flood basin inundation.

Individual channel belts typically were active for some 100 to 1000 years, whereas trunk channels (e.g., Oude Rijn in Fig. 1) could be active for multiple thousands of years (Stouthamer and Berendsen, 2001; Stouthamer et al., 2011). Repeated avulsions caused new river courses to form, leaving the old channel belt abandoned. The remaining alluvial ridges of such abandoned river courses were gradually buried by overbank sedimentation from the younger channels, which caused the ridges to lose their topographic expression over time (Fig. 2; Cazanacli and Smith, 1998; Van Dinter and Van Zijverden, 2010). The burial of older alluvial ridges was driven by relative sea level rise (RSLR) and upstream sediment supply. This burial took place relatively quickly in the beginning of the middle Holocene and gradually slowed down afterward, owing to declining RSLR (Van Dijk et al., 1991). In the downstream parts of the delta, aggradation decreased from ca. 1 m/ky around 5000 cal BP to ca. 0.3 m/ky around 2000 cal BP. In the central and upper delta, fluvial aggradation was ca. 0.8 m/ky around 5000 cal BP and ca. 0.3 m/ky around 2000 cal BP (Cohen, 2005; Stouthamer et al., 2011; Koster et al., 2016).

Owing to deforestation in the upstream catchment, the supply of fine-grained sediments — which levees typically are composed of — increased considerably in the youngest millennia (Erkens and Cohen, 2009; Erkens et al., 2011). Notably the contribution of silt in the supplied sediment remarkably increased (Erkens et al., 2013). Another distinct change is the increased frequency of large floods in the lower Rhine, particularly in the period 300–800 CE (Toonen et al., 2013, 2017; Cohen et al., 2016). The increased suspended load and higher flooding frequency together resulted in increased overbank sedimentation in the central and upper delta; here, aggradation rates were mainly controlled by sediment delivery from the upstream basin rather than by RSLR (Cohen et al., 2005; Erkens et al., 2011; Stouthamer et al., 2011). Increased sediment supply also resulted in the expansion of clastic sedimentation in upstream and in downstream directions over the last ca. 3000 years (Pons, 1957; Cohen, 2005; Gouw and Erkens, 2007). These developments concurred with channel network changes (Table 1; Berendsen, 1982; Stouthamer and Berendsen, 2001; Stouthamer et al., 2011) and anomalously large meander lengths in the rivers of the first millennium CE (Weerts and Berendsen, 1995; Stouthamer et al., 2011).

2.2. Natural levee characteristics

Natural levees form the upper part of alluvial ridges and constitute semicontinuous zones of relatively higher (1–2 m) terrain. They flank infilled residual channels and active channels and gradually slope downward toward the adjacent flood basins (Fig. 3A). Alluvial ridges of the Rhine typically have levees with dominant clay loam textures and are rich in calcium carbonate (Havinga, 1969; Weerts, 1996; Gouw, 2008). Their height and width are controlled by hydraulic and sedimentary conditions that act on a delta scale, such as the rivers' flood regime, upstream sediment delivery, and the delta plain geometry; (Fig. 3B). Levees incrementally grow in height until they reach an elevation that is overtopped by rare high floods only. Therefore, the crest mean height of a mature natural levee is attributable to regularly recurring floods (bankfull discharge), and local crest maxima are attributable to the rare highest floods (Filgueira-Rivera et al., 2007; Fig. 3A).

Crevasse splays are a specific type of overbank feature that forms in the flood basin when a levee breaches during floods. Although crevasse splays have a more complex sedimentological structure than natural levees (Smith et al., 1989; Farrell, 2001; Stouthamer, 2001; Shen et al., 2015), they can be lithologically and topographically difficult to distinguish, at least with the current data availability. This is because they can amalgamate with natural levees, which is especially the case in the upstream and central parts of the Rhine-Meuse delta where the levees are relatively wide and the density of alluvial ridges is high.

Levee height in the study area ranges from 0.5 to 1.5 m above the adjacent surface of the flood basins (Berendsen, 1982). Around the Rhine apex, levees are generally higher: 1.5–2.5 m (Erkens et al., 2011). Levees are typically 1–2 m thick where they overlie channel belt sands, a contact that is usually gradational (Allen, 1965; Berendsen, 1982). Where a levee overlies compaction-prone substrate next to channel belts (e.g., peat), its thickness can be up to 4 m (Makaske et al., 2007; Van Asselen, 2011), which is considerably larger than their topographic relative height.

In the Rhine-Meuse delta, natural levees reach some 50 to 500 m into the flood basin, measured from the channel belt edge (excess width in Fig. 3A). Lateral thinning of the levee deposits results in a gradual and diffuse transition between the levee and the flood basin (Fig. 3A; Weerts, 1996; Törnqvist and Bridge, 2002; Gouw, 2007). Natural levee width is determined by factors such as channel size and discharge, sediment supply, vegetation, substrate, and flood basin configuration (Fig. 3B; e.g., Törnqvist and Bridge, 2002; Adams et al., 2004). Vegetation roughness results in steeper decreasing stream-power gradients

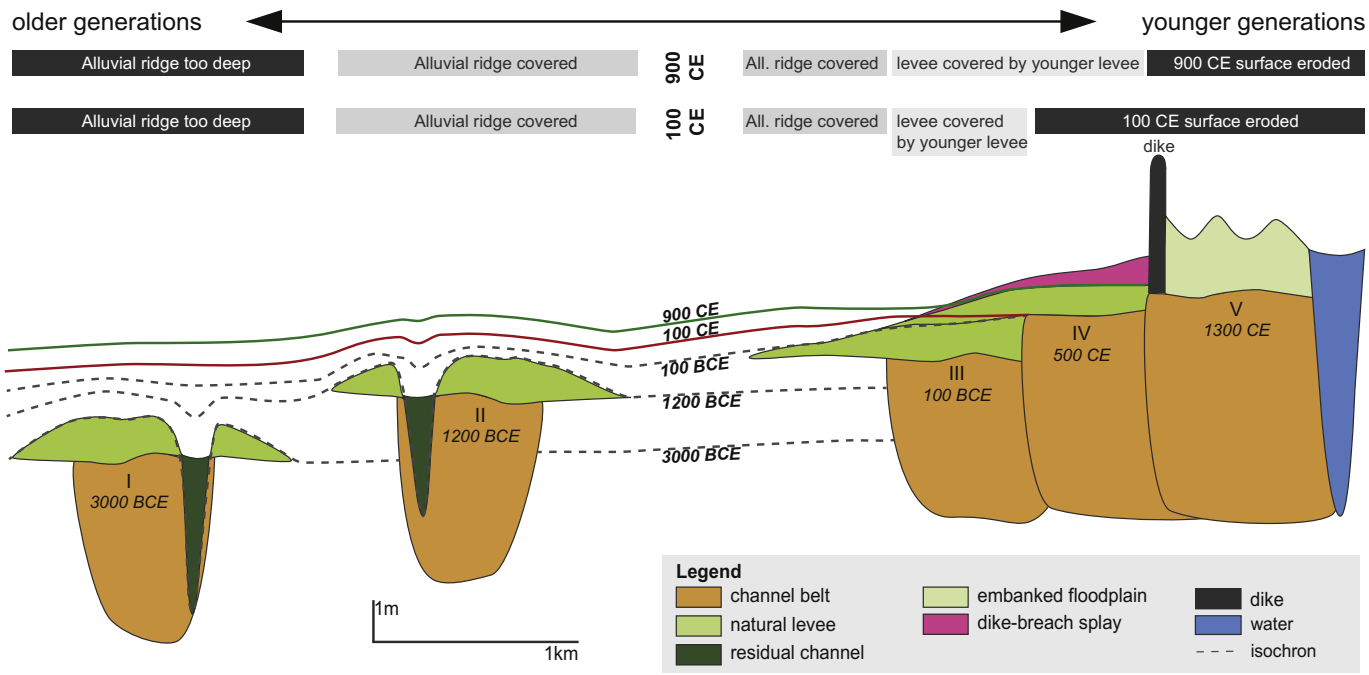

Fig. 2. Schematic cross section showing age-depth relations between generations of natural levee complexes and channel belts. Older generations of levees (I–III) get buried by continued accumulation of levee and nonlevee overbank deposits associated with younger channel belt generations and the flooding regime during their activity. The 900 CE surface roughly corresponds to the modern surface found in the LiDAR data, i.e., it matches the preembankment surface. Exceptions are the dike-breach deposits (post 900 CE) and artificial elements such as roads, dikes, etc.

Table 1
New avulsed rivers in the Rhine-Meuse delta between 500 BCE and 1000 CE compiled from overviews in Berendsen and Stouthamer (2001), Cohen et al. (2012, 2016) more specific references are given in the table; the start of the initiation and mature phases were inferred from radiocarbon dates and relative dating; location of the rivers is indicated in Fig. 1.

New river branch	Start of the initiation phase	Start of the mature phase
Nederrijn	ca. 500–20 BCE[a]	After 310 CE[a]
Linge	ca. 250–20 BCE[b]	After 20 BCE[b]
Hollandse IJssel	ca. 0–100 CE[c]	Before 800 CE[c]
Lek	ca. 40–300 CE[c]	Around 700 CE[c]
Waal	ca. 220–450 CE[b]	After 450 CE[b]
Gelderse IJssel	ca. 550–650 CE[a]	Around 900 CE[a]

[a] Based on Teunissen (1988, 1990); Makaske et al. (2008); Cohen et al. (2009).
[b] Based on Törnqvist (1993); Weerts and Berendsen (1995).
[c] Based on Berendsen (1982) and Guiran (1997).

from the channel to the flood basin, causing most sediment to be deposited close to the channel (e.g., Simm and Walling, 1998; Corenblit et al., 2007; Klasz et al., 2014), presumably resulting in narrow and steeper levees. Once formed, the levee relief in turn affects the local riparian vegetation patterns and flood hydraulics in its surroundings (i.e., by forming obstacles for flood flow; Fig. 3B).

When comparing multiple meanders within the same channel belt, levee shape tends to vary with meander geometry, rate of channel migration, local crevasse formation, and local interaction with pre-existent bank morphology and substrate (Fig. 3B; Hudson and Heitmuller, 2003). Downstream decrease in levee width over large distances has been reported for the Mississippi delta (Kolb, 1963), the Blue River USA (Lecce, 1997), and the Pánuco Basin, Mexico (Hudson and Heitmuller, 2003). These authors link this trend to downstream fining of sediment associated with a longitudinal sediment depletion and decreasing stream power because of the declining floodplain gradients. In the Rhine-Meuse delta, reconstructions by Gouw and Erkens (2007) and Erkens and Cohen (2009) showed a decrease in volume of overbank deposits by roughly a factor of 2 between the upstream and downstream end of our study area — matching the trends in the above-mentioned studies.

Steepness (i.e., cross-valley slope) is a function of levee width, levee crest height, and flood basin height (Fig. 3A). It can either directly be an important parameter for delta hydraulics and avulsion chances (Bryant et al., 1995; Heller and Paola, 1996; Mohrig et al., 2000) or more indirectly when compared to the downstream valley slope (Allen, 1965; Slingerland and Smith, 1998; Jones and Schumm, 1999). Although higher levees most likely favour initiation of avulsion, a critical threshold cannot be represented by one single value (cf. Törnqvist and Bridge, 2002) because avulsion triggering is affected by many other factors, such as flood basin topography (Aslan et al., 2005; Lewin and Ashworth, 2014; Toonen et al., 2016).

During and after deposition, only modest soil development took place in the levees because of their short periods of surface exposure in the dynamic sedimentary delta environment (Edelman et al., 1950; Van Helvoort, 2003). Ripening (i.e., initial soil formation; Pons and Zonneveld, 1965) already occurred during levee formation, repetitively after the waning stage of each flood. Compaction of underlying flood basin sediment and peat by levee loading mainly occurred while the levee formed, therefore ripening and compaction had only limited influence on the accuracy of the palaeo-elevation reconstructions in this paper. Surface lowering as a result of groundwater-table management since ca. 1000 CE has mainly affected flood basin areas (Havinga and Op't Hof, 1983). This caused occasional reexposure of buried alluvial ridges, but it has not significantly affected the elevations of the Common Era alluvial ridges as compaction had occurred already, mainly while the levees were forming. Only the distal parts of natural levees in the compaction-prone flood basins have lowered along with the subsiding flood basin surface, which hampers the reconstruction of past levee steepness.

3. Compiling and analysing the natural levee maps

3.1. Approach and materials

To assess the patterns of levee geometry through the delta, we

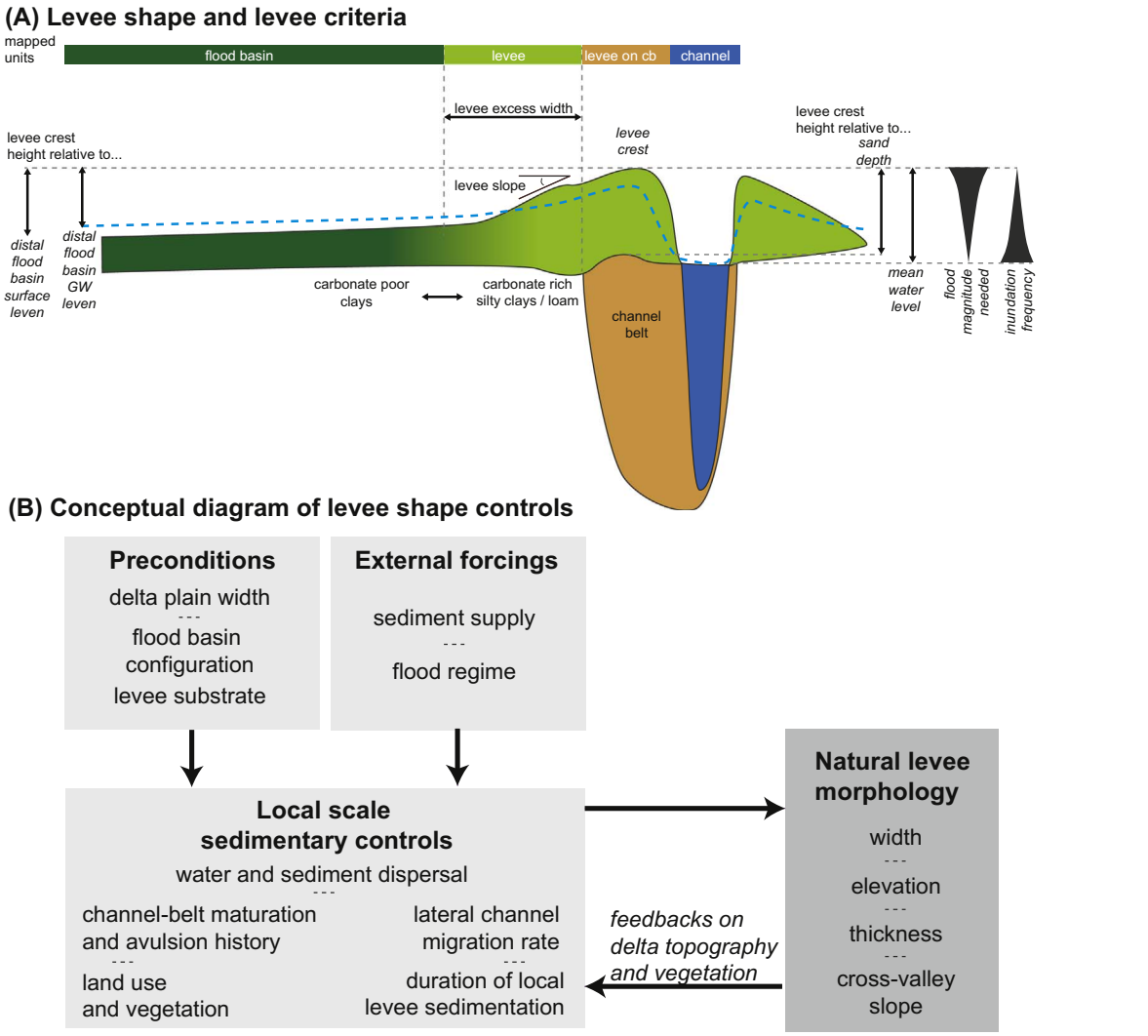

Fig. 3. (A) Levee shape and criteria. Idealised cross section of a channel belt and its levee in which the dimensions of levee shape are indicated. For levee width we primarily use lithological criteria; for height we use the elevation relative to the distal flood basin groundwater. (B) Conceptual diagram of controls on levee morphology. Natural levee morphology is influenced by local sedimentary controls that are in turn affected by natural preconditions, i.e., delta plain geomorphological setting (delta plain width, flood basin configuration, and substrate) and external forcings (flood regime, sediment supply). Delta plain setting determines how water and sediments are dispersed throughout the flood basins (e.g., by controlling flood amplitude, trapping efficiency). The substrate determines lateral channel-migration rate, controlling the duration of local levee sedimentation and thereby levee morphology. Channel-belt maturation and avulsion history control the location and pace of new levee formation. Vegetation and land use (e.g., deforestation) affect levee sedimentation patterns, e.g., dense vegetation can trap more overbank sediments close to the channel. When levee shape changes, the local relief changes as well as causing feedback on flood flow, vegetation patterns, and land use strategies.

established (i) maps of reconstructed geomorphology of the landscapes around 100, 500, and 900 CE, with the spatial distribution of natural levees and other elements in planform (Fig. 4); and (ii) two palaeo digital elevation models (DEMs) showing the topography of this levee landscape for 100 CE and 900 CE (Fig. 5).

For the two data sets, we developed methodologies to (i) integrate existing heterogeneous geomorphological data into new uniform maps, (ii) quantify burial depth of older levee surfaces where they are covered by younger and more distal overbank flood deposits, and (iii) determine whether buried older levee surfaces retained morphological expression at the time of reconstruction (Fig. 2). The essentials of the methods are described in this section, and details are contained in Appendix A.

The geomorphological reconstructions were compiled from several thematic base map layers, each containing the spatial extent and age of architectural elements in the delta subsurface (e.g., channel belts, levees). The levee base map is the primary base map in which the location and age of the levees were stored. In addition, base maps with the following architectural elements were compiled: (i) residual channel deposits that interrupt the levee cover on channel belts (Toonen et al., 2012); (ii) channel-belt sand bodies underlying levees (from Berendsen and Stouthamer, 2000; Cohen et al., 2012); (iii) outcropping sandy Pleistocene deposits (from Cohen et al., 2017a, 2017b); (iv) flood basin deposits (clay or peat facies: e.g., Van Dinter, 2013); and (v) dike-breach deposits (Tables 2 and 3; Fig. 2). These elements were mapped and stored in separate base map layers, and together with the levee base map, merged into the integrated geomorphological reconstruction maps (Appendix A2.2).

The maps were based on borehole queries, LiDAR data (Fig. 4C), and existing maps (e.g., soil maps, geomorphological maps, and palaeogeographical maps; Berendsen, 2007). For a complete description including resolution, coverage, scale, and references of the various types of data used in this study, the reader is referred to Appendix A1.

3.2. Geomorphological reconstructions

3.2.1. Mapping the levee extent

Based on general levee characteristics, three criteria were considered for identification of natural levees in the study area (Fig. 3A;

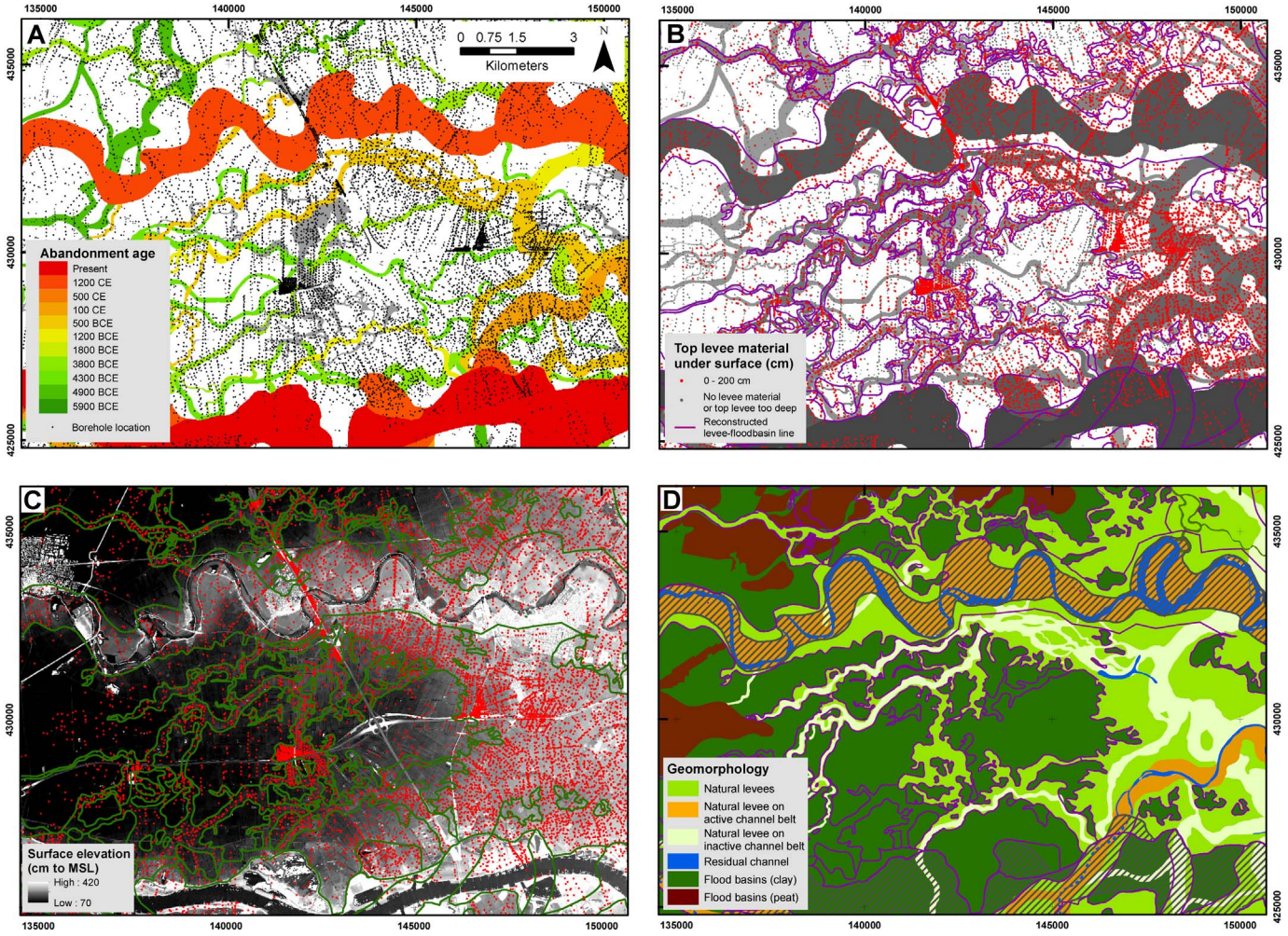

Fig. 4. Production steps in the natural-levee extent map. The location of the example area is indicated in Fig. 1. (A) High-density borehole data projected on the channel belt map of Fig. 1. This borehole data was the main source for the geomorphological levee map (B) Queried borehole results (presence levee/crevasse splay deposits) within 200 cm below the current surface and manually digitised boundary between floodplain and levee (purple lines, also in panels C and D) (C) LiDAR image used to refine the levee to flood-basin boundary derived from the borehole data. (D) Landscape reconstruction with the channel belt base map and levee base map combined, the diagonal line pattern indicates reworking by younger channels.

Table 2): (i) lithology: silty clay, clay loam, or loam; (ii) elevation relative to floodplain level: 1–2 m; and (iii) pedology: the levee material is calcareous. Distinguishing levees by carbonate content generally is less reliable as calcium carbonate was partly leached during later surface exposure; moreover, the criterion does not apply to the carbonate-poor natural levees of the Meuse. The use of elevation criteria can lead to diffuse boundaries when levees are wide and have low slopes. Levee boundaries also vary with the selected delta plain gradient. Therefore lithology was chosen as the most clear and objective primary criterion for levee identification.

To identify the boreholes with natural levees, we first queried the borehole database for the criterion ‘at least 40 cm thick layer of silty clay, clay loam and/or loam in the upper 2 m below the surface’ (Appendix A2.1). We then used LiDAR imagery, showing the shallow levees, as a secondary criterion (Berendsen and Volleberg, 2007; De Boer et al., 2008), to manually digitize the levee delineations from the borehole queries and the earlier maps (Appendix A1). Crevasse splays were treated as part of the natural levee complex as they are lithologically and topographically mostly indistinguishable on the considered scale.

3.2.2. Age attribution

Assigning the correct age to the mapped levees is important in order to trace their development and to link their activity to changing forcings such as changes in floods, sediment load regimes or phases of habitation. On-site age control was provided by over 300 ^{14}C dates (Berendsen and Stouthamer, 2001; Cohen et al., 2012; Van Dinter et al., 2017), ca. 70 sites with pollen records (e.g., Teunissen, 1988; Törnqvist, 1990), and numerous independently dated archaeological sites (e.g., Willems, 1986; Berendsen and Stouthamer, 2001). Because the presence and extent of architectural elements is relatively well known, relative dating methods provided further age constraints, for example by correlating features in detailed cross sections (e.g., Törnqvist, 1993; Weerts and Berendsen, 1995; Cohen, 2003; Gouw and Erkens, 2007). The combined architectural mapping and dating strategies are described extensively in Berendsen (1982), Törnqvist and Van Dijk (1993), Gouw and Erkens (2007); and further references in Table 3. The levees either overlying the channel belts or directly flanking them were assigned the age of the associated channel belt. We manually assigned begin and end ages of activity to the digitized polygon elements of the new natural levee base map. Similarly, we manually assigned ages to residual channel polygons in the second base map.

3.2.3. Time-sliced reconstructions assembled from base maps

To compile reconstructions of the natural levee landscape, the actively forming and the fossil levees (younger than 2500 BCE) were selected for 100, 500, and 900 CE based on their assigned ages. Levees of older channel-belt generations were presumed to lack any surface expression during the first millennium CE (Fig. 2 generation II and III). The < 2500 BCE criterion was chosen based on the levee surface

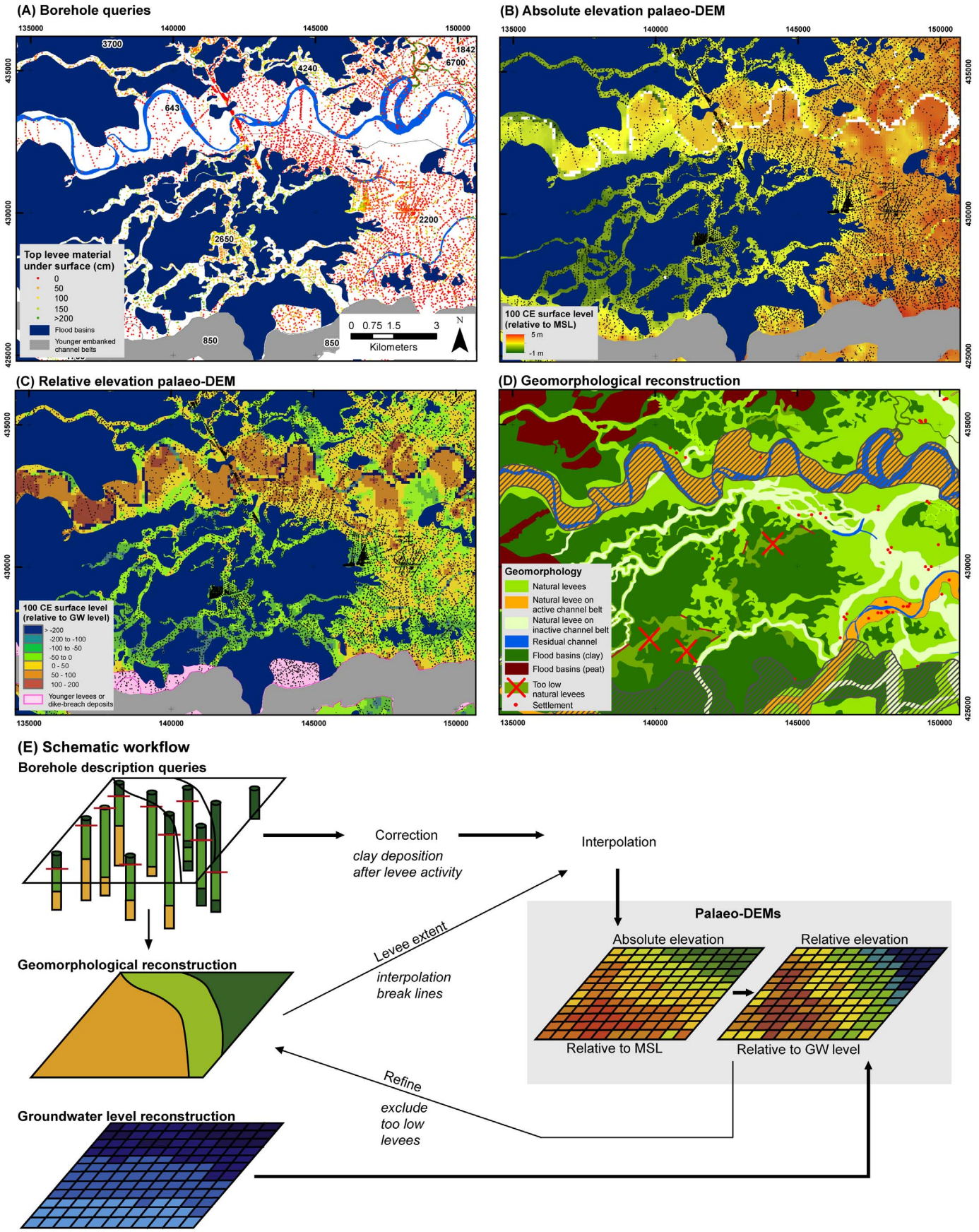

(caption on next page)

Fig. 5. Palaeo-DEM production steps, location of example area indicated in Fig. 1. (A) Source data for palaeo-elevation map: borehole database query results for the vertical position of the top of the levee (depth in the borehole) and age of the levee complexes (obtained from channel belt age maps Fig. 4A). The query results were corrected for burying flood-basin sedimentation after levee sedimentary activity (Appendix A2.3). (B) Elevation of the top of the levees (m OD). (C) Relative elevation of the top of the levees using a reconstructed groundwater surface 2000 cal BP as reference plane (Cohen, 2005; Koster et al., 2016). (D) Confrontation with natural levee extent mapping; dark tone alluvial ridges with red crosses indicate too deeply buried levees (> 2 m relative depth) — these are considered to have had no surface expression in the floodplains of the first millennium CE (also confirmed by absence of archaeological settlement finds from that period, red dots were taken from Pierik and Van Lanen, 2017). (E) Outline of the workflow of Fig. 5A–D, explained in a diagram.

expression of various levee generations inferred from delta-wide cross sections (Gouw and Erkens, 2007), this was later verified in Section 3.3. Furthermore, younger elements, such as eroding channels or a younger generation of levees, were removed from the reconstruction. Our GIS method is an extension of the approach described earlier in Berendsen et al. (2007) and Pierik et al. (2016) and is further outlined in Appendix A2.2.

3.3. Natural levee palaeotopography

3.3.1. Palaeo-DEM calculation

Once the levee extent was reconstructed for 100, 500, and 900 CE, we compiled two palaeo-DEMs (digital elevation models) for 100 and 900 CE. We started with the natural levee palaeotopography in 900 CE using the LiDAR elevation at the locations of boreholes where levees were encountered (i.e., within the levee landscape zones in Figs. 2 and 5). Where artificial landscape elements (e.g., roads, dikes, cities) were present, we used the original surface elevation derived from the original borehole description (for ca. 10% of the boreholes).

For the 100 CE palaeo-DEM, the vertical position (relative to the surface) of the top of the levee material was queried from the 70,000 boreholes (Fig. 5A). However, this does not directly represent surface level at a given time step, as clay draping has occurred after levee abandonment (Fig. 2). We therefore assessed distal clay deposition on top of the older levees by assuming a linear accumulation rate toward the 900 CE surface (this procedure is further outlined in Appendix A2.3). Both DEMs show landscape surface level relative to MSL. They were obtained by interpolating the reconstructed surface level at the borehole locations by quadratic inverse distance weighting using a maximum of 10 nearest points within a 2-km radius. The delineations of the levee to flood basin transition and of the residual channels from the geomorphological reconstructions were used as break lines for the interpolation procedure (Fig. 5B, E). In areas close to modern rivers, where deposits were formed by sedimentation of younger natural levees and dike breaches, we added a mask that highlights overestimation of the levee surface level (Fig. 5C).

3.3.2. Converting palaeotopography to relative elevation

The 100 and 900 CE DEMs (in m NAP; NAP = Dutch Ordnance Datum ≈ MSL) were normalised to the floodplain gradient, producing DEMs of relative elevation (Fig. 5C, E, Appendix A2.3). As the reference plane for normalisation, we used relatively smooth groundwater-level reconstructions for the first millennium CE (Cohen, 2005; Koster et al., 2016). These interpolated grids are a uniform delta-wide data set and have a vertical accuracy of ca. 13 cm (Cohen, 2005). These grids were considered more suitable than reference planes based on present-day surface LiDAR data, which suffer from differential surface lowering effects in downstream polders (e.g., Erkens et al., 2016) and post-embankment dike-breach fans that could cause elevation artefacts along modern rivers. The reconstructed groundwater surfaces are some decimetres below the average levee crest elevations, which is in agreement with soil formation observations (e.g., Edelman et al., 1950) and past human land use as inferred from archaeology (e.g., Willems, 1986). At the transition from levees to flood basins (relative elevation = 0), the water tables approximate the reconstructed surface level. To calculate the natural levee elevation relative to groundwater level at 100 and 900 CE, the groundwater level reconstructions for 2000 and 1000 cal years BP (50 BCE resp. 950 CE) were subtracted from, respectively, the 100 and 900 CE DEMs. For discussion of the accuracy of the resulting palaeo-DEMs, see Appendix A2.3.

Inactive channel belts that were abandoned before 2500 BCE were initially incorporated in the reconstructions (Section 3.3; Fig. 2). From the paleo-elevation reconstruction, we could then compare the vertical positions of these older levees relative to the reconstructed groundwater level. We considered natural levees that occurred deeper than 1 m below the reconstructed groundwater level as buried 'too deep' to have had full surface expression in terms of natural soil formation and human land use. Therefore, we manually labelled such areas as

Table 2
Lithology (USDA classification) and geometry of architectural elements in the Rhine-Meuse delta (adapted after Weerts, 1996; Hesselink et al., 2003; Gouw, 2008).

Architectural element	Lithology	Geometry	References
Channel-belt deposits	Very fine to coarse sand. Occasionally gravel and sandy-silty-clay. Fining-upward sequence.	5–10 m thick 50–2000 m wide	Berendsen and Stouthamer (2000); Cohen et al. (2012)
Residual-channels deposits	Peat, humic clay, sandy to silty clay. Sometimes sandy loam and fine sand.	1–3 m thick 10–80 m wide 0.5–10 km long	Havinga and Op't Hof (1983); Toonen et al. (2012)
Natural-levee deposits	Horizontally laminated silty clay, clay loam, or loam, occasionally with layers of clay or fine sand. Fining-upward sequences are common.	0.5–1.5 m thick, thicker toward the channel belt 50–500 m wide, flanking channel belt	This study
Crevasse-splay deposits	Silty clay, clay loam, or loam, channels: sand.	Splay: 1–2 m thick 0.1–5 km wide Channels (erosive): 1–8 m thick 0.1–10 km long 10–200 m wide	Smith et al. (1989); Makaske et al. (2007); Stouthamer (2001); Van Dinter and Van Zijverden (2010)
Flood-basin deposits	Thin laminated to homogeneous clay and humic clay. Vegetation horizons.	1–5 m thick 0.1–10's km wide	Havinga and Op't Hof (1983); Edelman et al. (1950); Steenbeek (1990)
Organic beds	*Alnus* or *Phragmites* peat, can contain up to 70% of clastic material (De Bakker and Schelling, 1989).	0.1–5 m thick 0.1–10 km wide	Pons (1992)
Embanked floodplain deposits	Very fine to very coarse sand, with clay or sandy clay layers. Fining-upward sequences are common.	5–10 m thick 200–1500 m wide	Hesselink et al. (2003); Cohen et al. (2014)
Dike-breach deposits	Sandy to silty clay, sand or gravel admixture. Occasionally with sand lenses.	0.5–1.5 m thick 0.1–3 km wide	Pons (1953); Berendsen (1982); Hesselink et al. (2003)

Table 3
Age attribution to the three sets of architectural elements in the Rhine-Meuse delta; TAQ = *Terminus ante quem* (date indicating minimum age), TPQ = *Terminus post quem* (date indicating maximum age).

Phase	Indirect dating	Direct dating	Potential errors	References
Channel belts and crevasse channels – Channel belt base map (Berendsen and Stouthamer, 2001; Cohen et al., 2012; and further updates)				
Begin (initiation, avulsion belt)	Deduced from dating flood basin organics, overlain by overbank deposits with nonerosive contacts (TPQ).	OSL from channels of avulsion-belt complex.	Time lag between accumulation of organics and burial by overbank clastics	Verbraeck (1970); Berendsen (1982); Törnqvist and Van Dijk (1993).
Activity (maturation)	From dating 'Begin' and 'End'. Also from archaeological dates: trapped water-bound archaeology or deduced from sites undercut by riverbank erosion (TAQ).	1) OSL from point bar facies; 2) ^{14}C on reworked material from bar facies or thalweg lag deposit (TPQ); 3) dating washed-in organics at contact point bar levee (TAQ).	1) Single ^{14}C dates of reworked material are often much older than the begin age; 2) OSLs show a bias toward the younger half of the period of activity, owing to river migration and reworking.	Berendsen (1982); Hesselink et al. (2003); Cohen et al. (2014).
End (abandonment)	Deduced from 1) base residual channels (TAQ) or 2) organics on top of flood basin deposits; 3) begin ages of upstream new-avulsed channels; 4) correlation to high-magnitude events.	1) OSL on plug bars and residual-channel associated point bar; 2) archaeology (TAQ).	Slow initial abandonment leading to delayed onset of accumulation of organic residual channel facies.	Verbraeck (1970); Berendsen (1982); Törnqvist and Van Dijk (1993); Toonen et al. (2012); Cohen et al. (2016).
Residual channel infills – Residual channel base map (this paper)				
Begin (base)	1) Adopting dates for end-of-channel belt activity obtained outside residual channels; 2) pollen-evidence from base of infill.	^{14}C date of base of infill.	Carbonaceous clay-gyttja organic sediment are susceptible for hard water effect — this can be avoided by picking riparian macrofossil for AMS ^{14}C dating.	Verbraeck (1970, 1984); Berendsen (1982); Törnqvist and Van Dijk (1993); Berendsen and Stouthamer (2001).
Activity (silting up)	1) From dating 'Begin' and 'End'; 2) pollen evidence from within infill; 3) change of infill facies correlated network change.	1) ^{14}C date in infilling; 2) archaeology in infilling; 3) recognising event-beds major floods in infilling.	Reactivations by crevasse and chute channels, cause hiatuses in the infill.	Teunissen (1988); Törnqvist (1990); Hoek (1997); Toonen et al. (2012); Toonen et al. (2013); Minderhoud et al. (2016); Cohen et al. (2016).
End (top)	Soil horizons or archaeological layers in top of the fill.	^{14}C date top infilling (TAQ).	Final stages of lacustrine infill very local and diachronic over the residual channel element.	Verbraeck (1970); Berendsen (1982); Törnqvist and Van Dijk (1993); Hoek (1997).
Natural levees and crevasse splays – Natural levee base map (this paper)				
Begin (initiation, avulsion belt)	Deduced from dating flood basin organics, overlain by overbank deposits with nonerosive contacts (TPQ).	Buried archaeology (TPQ).	Time lag between accumulation of organics and burial by overbank clastics.	Verbraeck (1970); Berendsen (1982); Törnqvist and Van Dijk (1993).
Activity (maturation)	Pollen in levee deposits (TAQ).	Archaeology within levee deposits (TAQ).	Levee preservation bias to younger half of activity period, owing to river migration and reworking — affects long-lived largest river channels mainly.	Verbraeck (1970); Berendsen (1982).
End (silting up)	1) Deduced from associated res. channel 'Begin' dates (TAQ); 2) by adopting channel belt 'End' dates (TAQ).	Archaeology in the top of the levee deposits (TAQ).	Early abandonment stages of channel belt (narrowing channel) may be last pulses of levee aggradation, especially near bifurcations.	Verbraeck (1970); Willems (1986); Berendsen (1982); Törnqvist and Van Dijk (1993); Van Dinter (2013).

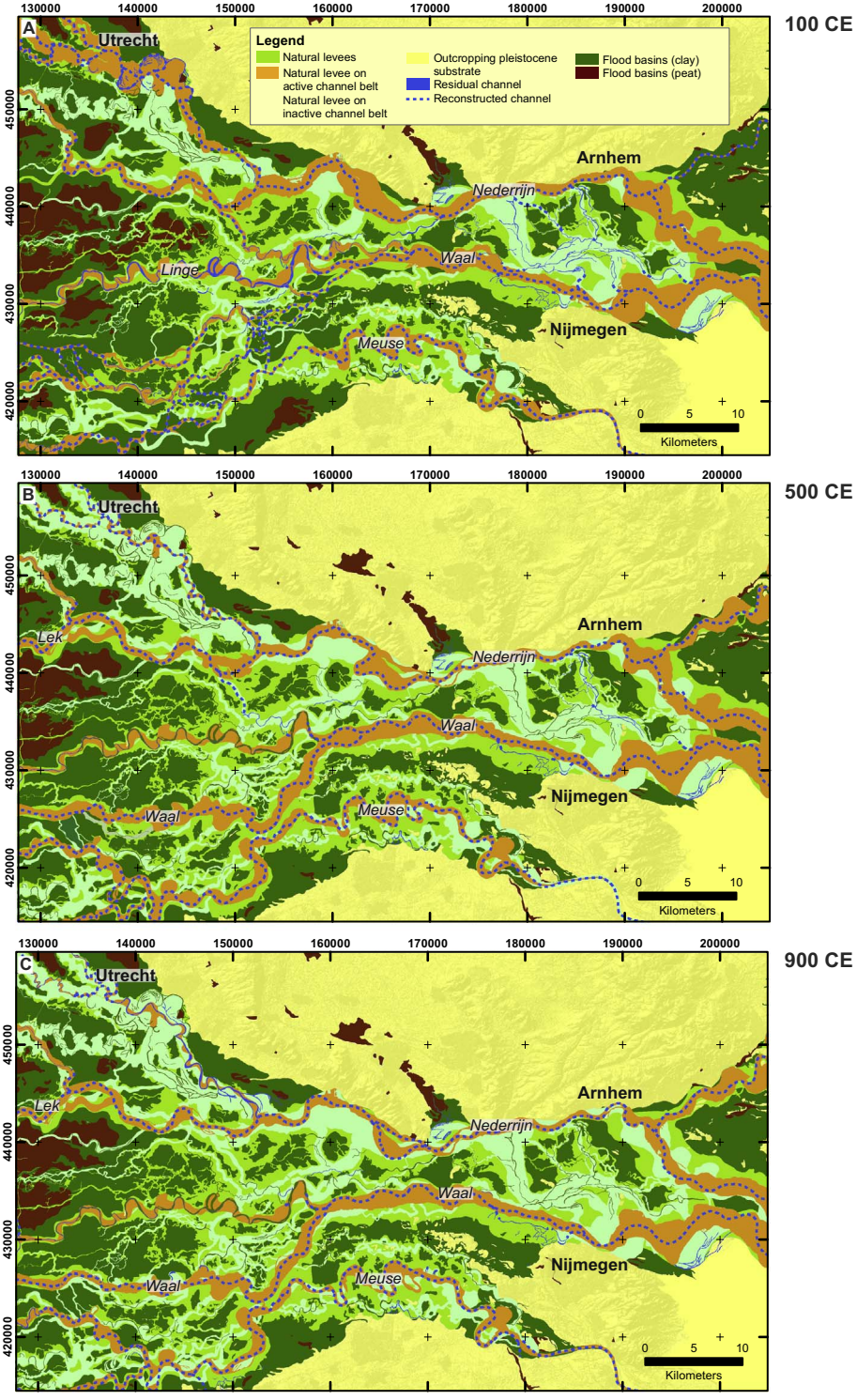

Fig. 6. Geomorphological reconstructions for 100, 500, and 900 CE for the central and upper Rhine-Meuse delta (Fig. 1); see Appendix B for larger files.

'inactive' in the levee base map (red crosses in Fig. 5D) and subsequently repeated the procedure in Section 3.2.3 to update the levee extent of the geomorphological map resulting in Fig. 6. The too-low top of these levees is confirmed by the absence of Roman settlements on these locations (Appendix B).

3.4. Regional-scale analysis

Based on the map products, we divided the delta into three main segments: (i) a narrow upstream segment with wide levees and narrow flood basins (U1–U4), (ii) a widening middle segment containing multiple channel belts with abundant and wide levees (C1–C4), and (iii) a wide downstream segment (D) with wide flood basins and narrow levees (Figs. 6–9). Within these segments we made a further subdivision based on our newly mapped characteristic levee morphology, e.g., levee surface area, average alluvial ridge elevation (Fig. 10). For each delta segment we quantified the areal cover, the average elevation, and the variation in elevation of the levee landscape. We additionally isolated 13 single-generation channel belts throughout the delta (indicated with white lines in Fig. 9), of which we derived metrics on levee width, asymmetry, and relative elevation. Width and asymmetry in width were inferred by comparing excess levee widths (i.e., distance from the

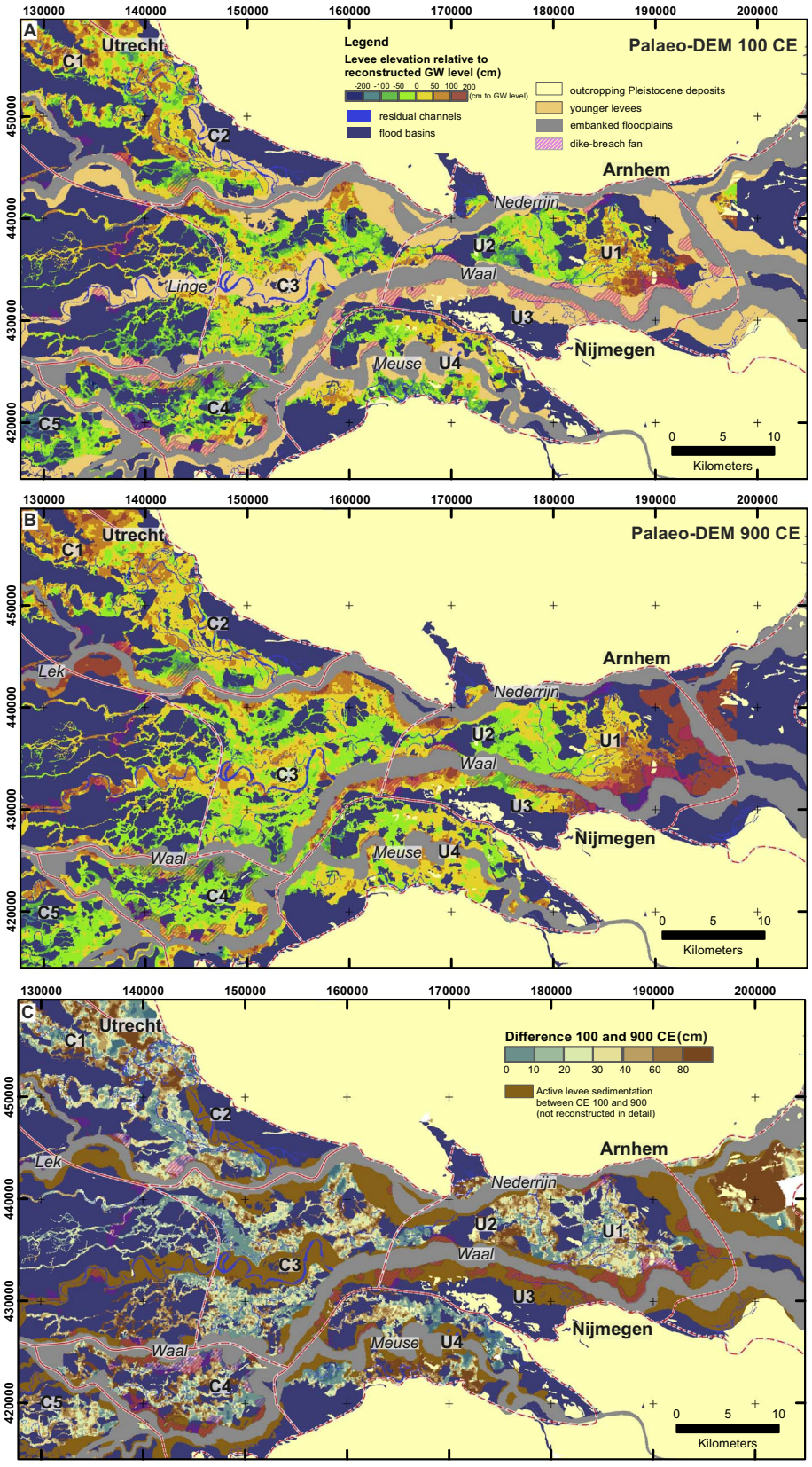

Fig. 7. Palaeo-DEMs for the central and upper Rhine-Meuse delta (Fig. 1), showing the relative elevation of the natural levees at (A) 100 CE (0 m = groundwater level 2000 BP) and (B) 900 CE (0 m = groundwater level 1000 BP), and (C) the elevation difference of the levees between 100 and 900 CE. See Appendix B for larger files.

channel belt to the flood basin; Fig. 3A) measured every downstream kilometre. After quantifying these differences in levee shape, we compared these across the entire delta to the independently reconstructed controls (e.g., flooding regime, sediment supply, avulsions) that varied during the studied period. From this comparison the levee-forming processes were inferred.

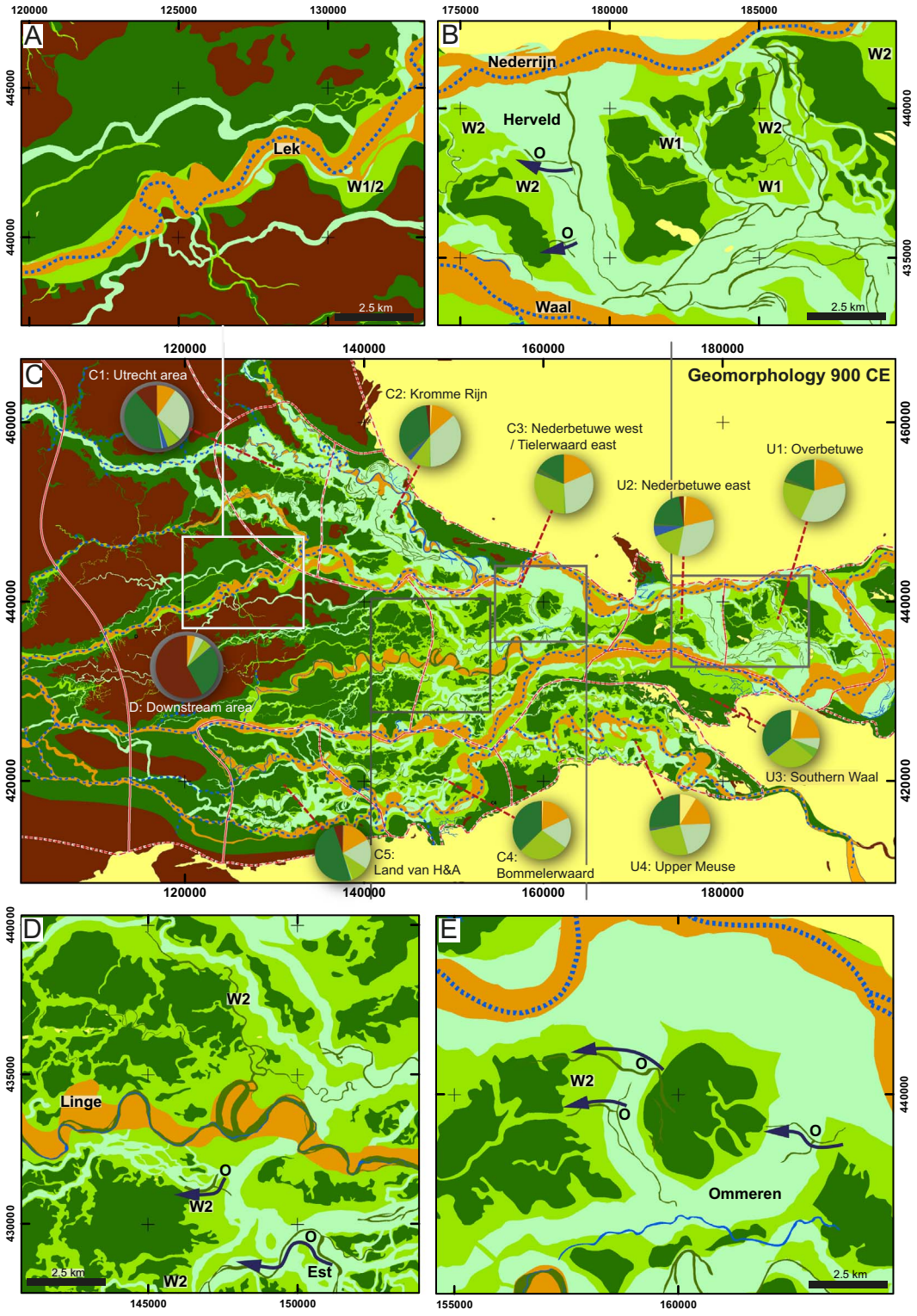

Fig. 8. Geomorphological reconstruction for 900 CE, with pie charts indicating areal proportions of landscape units per segment, for legend see Fig. 6A. O = overflow channel, W1 = wide levee/crevasse splay in the upstream part of the channel belt, W2 = wide levee flanking S-N oriented channel belt, forming in line with regional westward sloping delta plain gradient.

4. Spatial and temporal variations in levee geometry

4.1. Delta-wide longitudinal trends

In the upstream part of the study area (segment U1), relatively high levees (1–2 m) are present in the 100 and 900 CE reconstructions (Figs. 7AB and 9B). This is also the area where delta plain width decreases in the downstream direction from 30 km around the apex to 13 km in segment U1 (Fig. 1 and red triangle 1 upstream in Fig. 9B). Going downstream, around U2 and U3 the delta plain becomes wider again (from 13 to 20 km) coinciding with lower levees elevated on average 20–30 cm in U2. In the downstream part of U2 narrowing occurs (20 to 9 km; Fig. 9B, red triangle 2); this corresponds to levee heights of 0.5–1 m around the narrow part downstream of U2. We

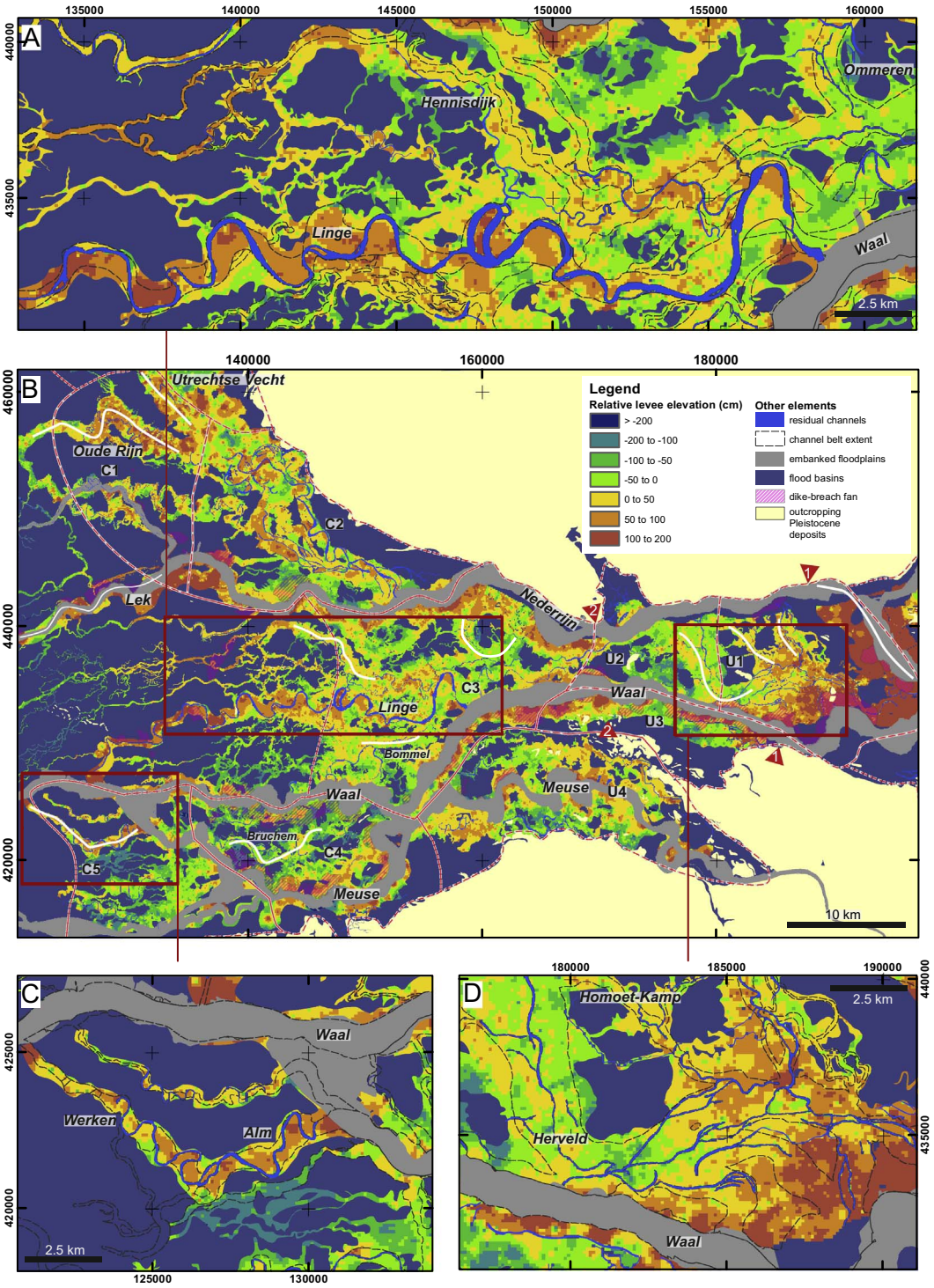

Fig. 9. Examples of relative levee elevation 900 CE. White lines indicate the channel belts that were analysed on levee-excess width, the red triangles indicate the two reaches of delta-plain narrowing. (A) and (C) show examples of variation in levee height on a meander-belt scale. (B) Overview of natural-levee relative heights across the delta (calculated above surrounding flood basin mean groundwater level). (D) Zoom to the confined flood basins of the upper delta, with their high, accentuated levees. The names of channel belts discussed in the text are indicated.

interpret the high levees as products of relatively higher flood water levels that formed when flood propagation was hampered when floods reached the narrowing of the delta plain in segment U1. The amplified flood levels allowed overbank sedimentation to reach relatively high elevations, resulting in higher natural levees above the regional groundwater level. In U1, flood amplitudes were likely further increased by three N-S oriented alluvial ridges that hampered flow in the delta plain (Fig. 8B, C). The levee heights indicate that the typical morphology-forming flood would have reached 0.5–1 m higher in the narrow segments compared to wider segments (U2) and segments farther downstream.

The average cover of the alluvial ridge area in our maps ranges from 67% in the upstream sections (U1–U4), to 62% in the central delta (C1–C5), to 14% in the downstream part (D). Segment C3 proportionally contains the most levees and crevasse splays (75–80% of 314 km^2; Fig. 8C). Roughly 75% of the levees in this segment date from rivers

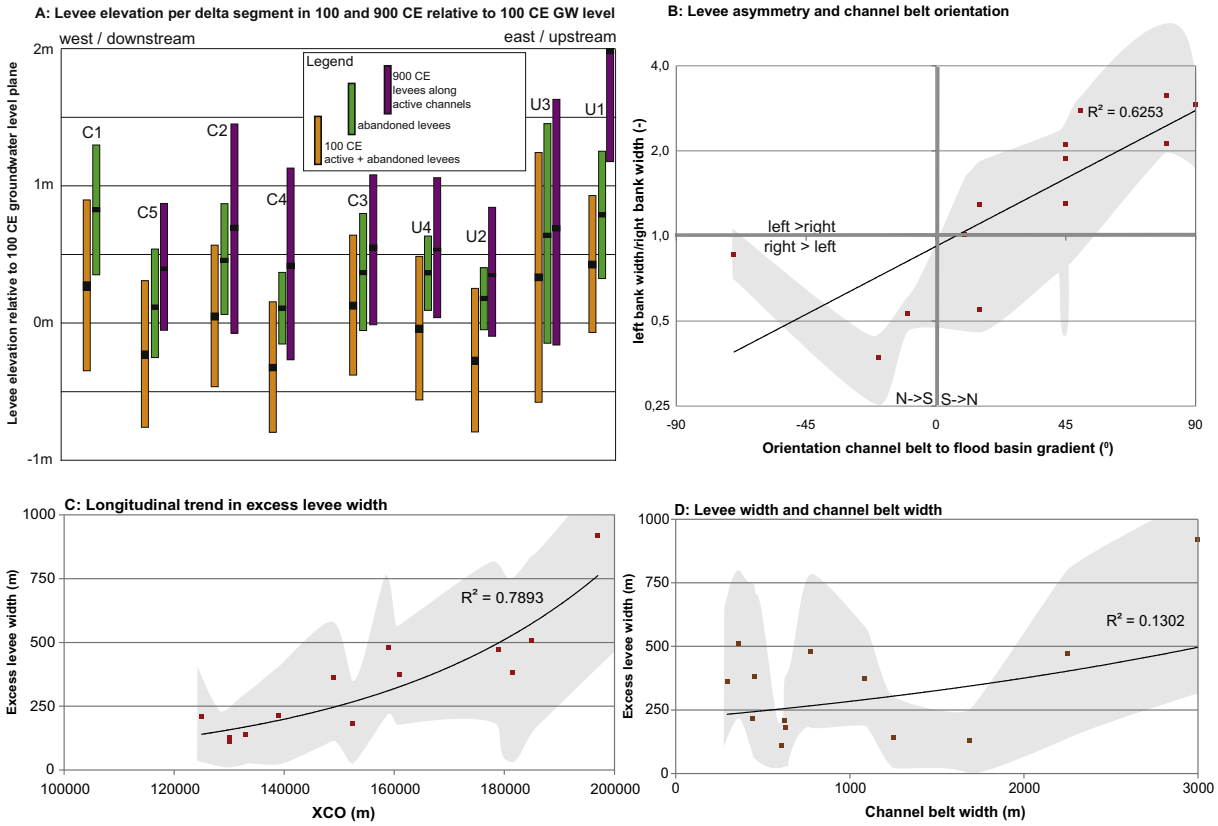

Fig. 10. (A) Levee elevation per delta segment in 100 CE (yellow bars) and 900 CE (green bars: all levees; purple bars: active levees only) relative to the 100 CE groundwater level; see also Table A.4. (B)–(D) Show metrics of levees along 13 channel belts throughout the entire delta (indicated in Fig. 9), grey shades indicate a spread of one standard deviation. (B) Levee asymmetry is a function of channel-belt orientation: a larger angle of the channel belt relative to the flood-basin gradient yields more asymmetric levees (wider larger downslope). (C) A clear trend is observed in longitudinal position of a channel belt (mean position of the x-coordinate was taken) and the average levee width along the channel belt. (D) A weak relation is found between channel-belt width and excess-levee width.

that were active during the last millennia BCE, which caused this segment to be a relatively high part in the delta from the first millennium CE onward (Fig. 7AB). The abundant levees can be seen as the result of repeated avulsions and failed avulsions known to be concentrated in this area (Stouthamer, 2001; Bos and Stouthamer, 2011), associated with neotectonic subsidence downstream of the Peelblock and Peel Boundary Fault Zone (Fig. 1; Berendsen and Stouthamer, 2000; Cohen et al., 2005; Stouthamer et al., 2011).

Levee-excess width decreases in a downstream direction (both average width and spread in width; Figs. 6 and 10C), also the boundaries from levee to flood basin become sharper in a longitudinal direction. In our results, the relation between average levee-excess width and downstream position in the delta was relatively strong (R^2 = 0.79; n = 13 – Fig. 10C). This implies that downstream position is the most dominant predictor for average levee width along a channel belt; in our case it is more important than channel-belt width (Fig. 10D; R^2 = 0.13). The abundancy of levees in the upstream and central parts of the delta combined with their decreasing widths suggests that coarse-grained overbank deposits were probably relatively efficiently trapped here.

4.2. Levee development between 100 and 900 CE

Avulsion during the first millennium CE caused levee depocentres to shift: the new river courses replaced flood basin areas with levees, increasing their areal portion from 57 to 64% of the total area in the C and U segments. Routing of the new channels was determined by the levee topography in the delta; it explains the position of the new river Waal, which was diverted around area C3 toward the low-lying segment C4 (compare Fig. 7A and B). Development of avulsions within the enclosed basins was limited because splay development was blocked by a neighbouring channel belt (cf. Toonen et al., 2016). Clay draping on fossil natural levees (i.e., of the inactive channel belts) at more distal positions from the active channels raised these levees by a few decimetres over the studied period (39 ± 32 cm on average delta-wide). The clay layer on the higher fossil levees was thinner than on the lower levees and the flood basins, causing topographical levelling (Fig. 7C). No downstream trend was found in the amount of clay deposited on the fossil levees in this study (compare orange and green bars in Fig. 10A). The topographical levelling of the old levee landscape contrasts with the high new levees along the active channels. As an example, in section U3 and along the river Lek in section C2, the new levees locally appear about a meter higher compared to the levees of their precursors (Figs. 7, 9, and 10A).

4.3. Trends along individual channel belts

Levee width varies considerably along individual channel belts, regardless of longitudinal position, age, or channel-belt width (Figs. 6–9, Appendix B). Remarkably, levee width of N-S oriented alluvial ridges is asymmetric, the most notable cases in the upper and central delta are indicated as W2 in Fig. 8. The levees on the western side of these channel belts are 500 to 1500 m wide, whereas those on the eastern side are at most a few hundreds of metres wide. This asymmetry changes with channel-belt axis orientation relative to the E-W trending delta plain slope (R^2 = 0.63; n = 13; Fig. 10B). This relation was found in all segments of the delta, although less pronounced at first sight downstream where levees are less wide. The preferential overbank sediment transport in the direction of the overall delta plain slope indicates that levee dimensions were controlled by flow patterns

in the flood basins. They most likely formed during a high flood stage when flood basin throughflow was established. In the upstream and central segment (C3), the presence of these N-S directed channel belts caused the flood basins to be enclosed. During floods, breaching of these N-S oriented channel belts created E-W oriented overflow channels (e.g., Est, Ommeren; dark blue arrows in Fig. 8D, E; Havinga and Op't Hof, 1983), again showing that considerable flow occurred in these flood basins, at least during the most severe floods of the first millennium CE.

Generally, levee complexes tend to be widest in the upstream parts of channel belts, i.e., just downstream of their avulsion points (500–1500 m; indicated with W1 in Fig. 8A, B). Most likely, these features formed as multichannel avulsion belts during the initial stage of channel-belt activity (Smith et al., 1989; Stouthamer, 2001; Makaske et al., 2007), rather than representing levees from the single-channel mature phase of these channel belts. The avulsion belt deposits are especially well-preserved along relatively narrow and short-lived channel belts.

Within single channel belts, significant differences in elevation occur. Generally, levees on top of channel belts are highest (compare elevation inside and outside channel belts, black-dotted lines in Fig. 9), but when they overlie flood basin deposits they can also be relatively high. Where residual channels have preserved as pronounced meanders, the data set allows us to compare levee size along the inner bends (e.g., covering point-bar channel deposits) and along the outer bends. Levees in the inner bends of meanders are relatively high (1 to 1.5 m), whereas along the outer bend levees are narrow and lower (around flood basin level and max. 100 m wide; e.g., Linge, Alm/Werken channel belts in Fig. 9A, C). The lower and narrower levees on the outer bends appear to contradict the hydraulic concept of cross-channel water-level setup toward the outer bends owing to flow momentum, which would generate higher and wider outer bend levees (Leopold and Wolman, 1960; Hudson and Heitmuller, 2003). The causes of higher levees in the inner bends compared to the outer bends can be sought in (i) topping up of the original levees with additional silty sediments as an abandonment overprint, in the final stages of ephemeral flow activity, in a narrowing channel, and at reduced flow velocities (e.g., Toonen et al., 2012; Van Dinter et al., 2017); and (ii) post-depositional compaction of flood basin sediments underlying the outer bend levees (e.g., Van Asselen, 2011). These mechanisms can explain the differences in height between the inner and outer bends. The controls behind the narrow outer-bend levees, however, remain to be further explored.

5. Discussion

5.1. Controls on natural levee shape

In the previous section, we have seen that the levee dimensions vary throughout the delta and over time, driven by changes in hydraulic and sedimentary processes. This discussion section builds on this by formulating hypotheses on the relative importance of natural preconditions (delta plain width, substrate), external forcings (variation in discharge and sediment load; Figs. 3B and 11), and downstream trapping that controlled levee shape in the first millennium CE.

5.1.1. Role of natural preconditions

Our results strongly suggest that levee dimensions were not solely determined by the flooding regime and channel dynamics of the Rhine branches. They were also controlled by conditions occurring in the inundated flood basins. The higher levees that formed in the narrow parts of the delta are a clear example of this. The inference that in our case the narrowing of the upper delta floodplain caused higher flood amplitudes differs from studies on levee morphology carried out in more confined valley systems of a few kilometres wide (e.g., Magilligan, 1985: Galena River, USA; Lecce, 1997: Blue River, USA; Kiss et al., 2011: Danube River, Hungary). In these examples, floodplain narrowing, besides raising the water level, also led to increased stream power, keeping sediments in suspension, and subduing overbank aggradation (i.e., keeping the levees relatively low). In the 1 to 2 km wide reaches of the anastomosing Columbia River valley (Canada, Filgueira-Rivera et al., 2007), confinements also caused significant flood heights and flow velocities, which limited levee width but allowed them to aggrade relatively high and to become relatively steep. In the Rhine-Meuse delta, the narrowed reach of the delta plain is a factor 10 wider than the valley examples, and additionally the upstream segments contain alluvial ridges that cross over the entire delta plain (i.e., compartmentalisation of the delta plain). These differences in natural preconditions caused the through-flow velocities in the flood basins (i.e., stream power) in the upper Rhine-Meuse delta to be less strongly raised compared to the valley examples. Numerical hydraulic modelling could further test the critical levels of delta plain narrowing, valley gradient, and obstacle height (alluvial ridges) that cause levees to grow higher or cause their development to be subdued by overflow. Such studies can use the reconstruction maps as realistic input topography to further test the basic principles of delta plain width and floodwater level and its implications for overbank sediment dispersal and deposition.

Another natural precondition that influenced levee geometry is the substrate adjacent to the channel belt and underlying the levee (Figs. 2B and 11), especially in the more downstream segments where the levees overlie compacted peat. Subsidence of the underlying peat in response to loading with levee sediment created extra accommodation space for overbank sedimentation (Van Asselen, 2011). Furthermore the erosion-resistant properties of peat retarded channel-bank erosion and hence caused the channel position to be fixed (Makaske et al., 2007) and levee sedimentation for long periods at the same place. Subsidence and channel fixation combined resulted in narrow but rather thick levees that did not become very high.

5.1.2. Role of external forcings changing over time

Especially in the upstream parts of the study area, the crests of the youngest levee generations, formed along newly avulsed main river branches, are clearly higher (0.5 to 1 m above groundwater level in segments U1, U2, U4, and C2; Fig. 10A) than levees along similar-sized precursor channels. This is in part the result of the interaction of floods with the delta plain width and compartmentalisation described above. The high elevation of the younger levees may be additionally attributed to the greater availability of suspended sediments in the first millennium CE compared to the millennia before (Fig. 11; Erkens and Cohen, 2009; Erkens et al., 2011) and the intensified flood regime after ca. 250 CE observed by Toonen et al. (2013, 2017). The observation that the volume of overbank sedimentation in levee complexes and flood basins (Erkens and Cohen, 2009) increased by a factor of 1.6 to 2 from the last millennia BCE to the first millennium CE supports the idea that the young levees are larger because more levee-building material was supplied (especially the silt fraction of the suspended load; Erkens et al., 2013). To explain the relative higher elevations, however, frequent high flood levels also are required as has been suggested for other river settings (Filgueira-Rivera et al., 2007). This principle is confirmed by our data: the 900 CE levees were formed in a period of increased frequency of large and moderate flooding of the Rhine, which locally caused levee crests to become ca. 1 m higher relative to the flood basin compared to their processors. The levees in the 100 CE landscape were lower as they had not experienced these large floods. Delta-wide, when comparing the average elevation of the entire levee area (i.e., from the flood basin limit to the channel, so not only the highest crests; Fig. 2A) the differences between the 100 and 900 CE levees are smaller (compare yellow and purple bars in Fig. 10A). This indicates a large spread in elevation within the youngest levee generation. Besides the levees, also the flood basins silted up (especially the lower parts by ca. 50 cm) aided by the increased sediment supply (Fig. 11). The occurrence of severe floods is not regarded as important for the filling of the lower parts of the flood basins as it is for levees. This is because the lower

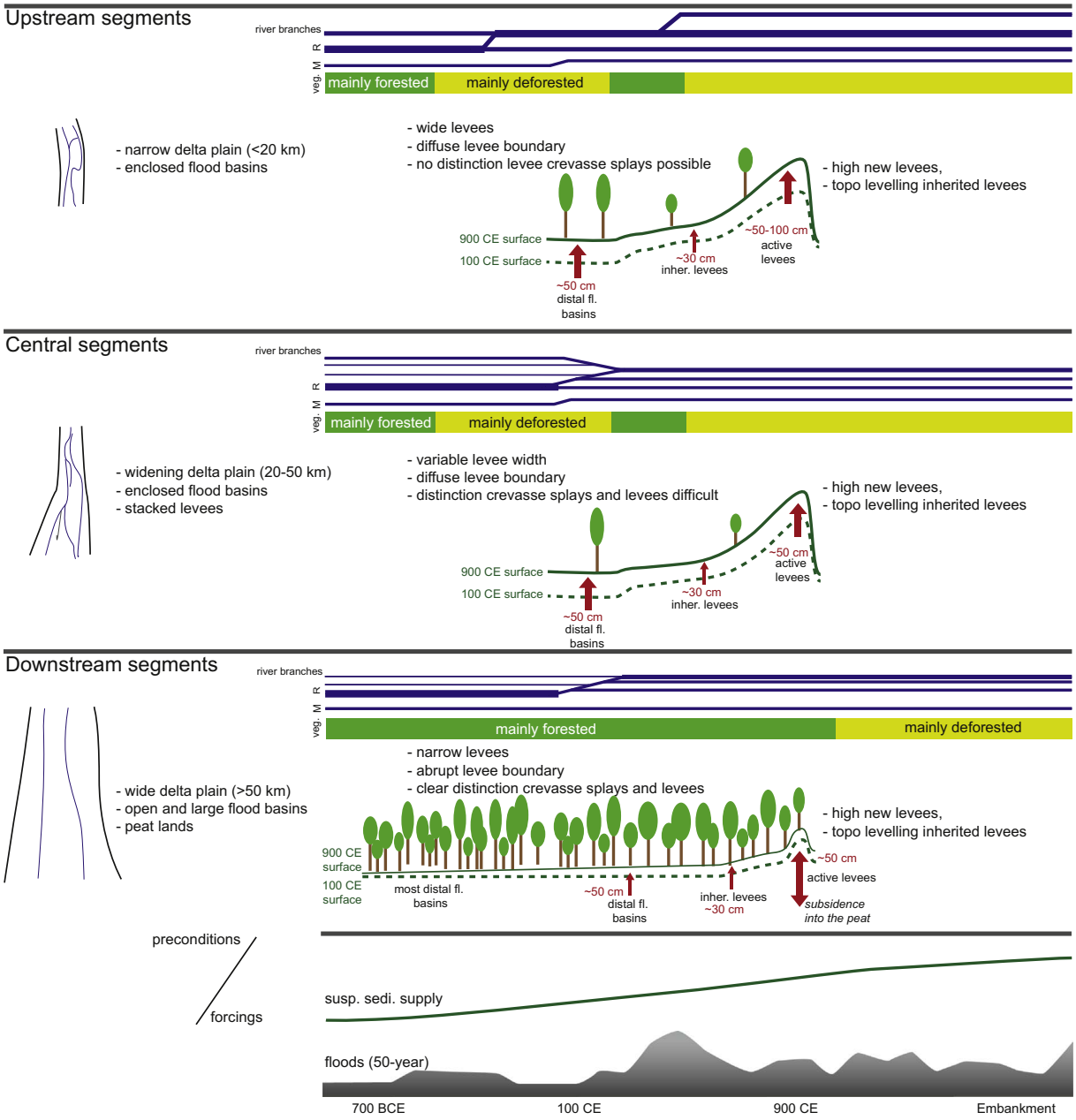

Fig. 11. Conceptual diagram on levee shape evolution during the first millennium CE throughout the Rhine-Meuse delta. Suspended sediment supply from Erkens and Cohen (2009), 50-year flood recurrence floods from Toonen et al. (2013). Levee width after Figs. 8 and 10C, riparian vegetation after Teunissen (1988) and Kooistra et al. (2013). Sedimentation rates of levees and fossil levees from Fig. 10A, in distal flood basins after Gouw and Erkens (2007). Active river branches (R = Rhine, M = Meuse) after Berendsen and Stouthamer (2000).

flood basins were also inundated during lower or modest magnitude floods. Therefore, sediments will have reached the flood basins via crevasses and lower parts of the levees regularly (e.g., Makaske et al., 2002; Filgueira-Rivera et al., 2007).

The higher levees along the new branches possibly induced feedbacks on channel morphology and avulsion probability. Considering channel morphology, previous studies have noted that the rivers of the first millennium CE developed larger meander wavelengths than their older counterparts (Weerts and Berendsen, 1995; Berendsen and Stouthamer, 2000), suggesting that these rivers could route more discharge through the river bed than their precursors. One can explain this increase in bankfull discharge carrying capacity as a consequence of the raised levees along the channels. Following this explanation, no major changes in mean annual discharge supply to the delta would be required to generate such meander wavelengths. When the levee elevation increased relative to the flood basin, while the levee did not become much wider, the cross-channel slope probably increased, accelerating avulsion. For example, the Waal and Meuse avulsions (Table 1) along either side of segment C4 (Fig. 6C) could have been aided by the levee superelevation at their avulsion points. However, the wide spread in elevation implies the presence of lower parts of the levees sensitive to overtopping, which raises the question whether these highest crests really determined avulsion chances in our case.

5.1.3. Sediment trapping and role of vegetation

The narrowing of levees from the upstream to the downstream parts of the delta matches the downstream volume reduction of late Holocene levee and crevasse splay deposits (Gouw and Erkens, 2007; Erkens and Cohen, 2009). The preserved volume per square kilometre of silty clays and clay loams was reconstructed to be two times less in the downstream part compared to the upstream part of the delta. In comparison, volumes of flood basin clay as distal overbank deposits are rather

evenly distributed between the upstream, central, and downstream parts of the delta. The upstream deltaic reaches apparently were relatively more efficient in trapping silt fractions (and probably also the finest sand fractions) than in trapping clay. A longitudinal decrease in levee size has been observed in other river systems as well where it has been explained by a downstream decrease in availability of suspended material (i.e., the sediment concentrations of flood water leaving the channel; Kolb, 1963; Hudson and Heitmuller, 2003; Thonon et al., 2007). Our findings imply that the loss of sediment to levee building in upstream reaches is the reason that the excess levee width drops so strongly in downstream sectors. The occurrence of abundant flood basins enclosed by alluvial ridges in the upstream and C3 segments is a likely setting to promote the high trapping efficiency for the silt fraction. In these areas the fossil alluvial ridges (i) slowed down the flow of incoming water that overpassed the alluvial ridges; and (ii) prevented floodwater outflow when the water levels in the flood basin started to drop in the final stages of the flood, allowing clays but also relatively much silt and the finest sand fractions to settle. While the absolute amount of sediments available for levee formation decreased in a longitudinal direction, the downstream levee width trend was likely enlarged by a positive land use feedback concerning riparian vegetation (Fig. 11). The large areal coverage of alluvial ridges in the upstream and central delta were attractive places for people to live (Pierik and Van Lanen, 2017), leading to deforestation of the area since ca. 500 BCE (Teunissen, 1988). The absence of a dense riparian vegetation resulted in a smaller lateral flow velocity gradient of the overbank flow, facilitating overbank fines to be conveyed farther into the flood basin. This deposition further expanded the levee area in the upper and central delta segments. Once larger amounts of coarse-grained sediments could reach the flood basins, the levees became wider and the transition to the flood basin became more gradual. In the downstream parts of the delta, marsh and swamp vegetation remained largely intact (Kooistra et al., 2013), and interactions of flood dynamics with vegetation were more natural. As a result, the flow velocity gradient from the channel toward the flood basin would have been steeper here, generating narrower levees. This may well explain the occurrence of the remarkable narrow outer bend levees in the peatlands in Fig. 9A, C; trapping by vegetation in the flood basin would then be more important than channel hydraulics.

5.2. Map information value, potential, and implications

In our data-driven geomorphological approach we reconstructed and analysed a palaeo-levee landscape of which much data is available at the scale of an entire delta. By quantifying the levee characteristics from these reconstructions in a uniform way across the entire delta, our map products allow assessing the role of regional flood basin configuration, delta confinement, and spatially varying flood amplitudes on levee shape. This section discusses the benefits and limitations of our methodology and gives recommendations for further research.

In the reconstructions, the location and extent of the levees are generally known within tens of meters to maximal hundreds of meters owing to the availability of > 100,000 lithological borehole descriptions and abundant map data sets. For more detailed use, e.g., to study levee width for smaller levees, it is important to have a clear definition of the distal levee boundary in the mapping. We considered this as the line where modestly inundated flood basin water tables (i.e., the regional groundwater reconstructions) intersected the levee relief rather than a particular break or convexity in transverse slope.

The precision of age control of the mapped levees varies across the study area. It was based on some 300 dates from site locations, from which the ages were transferred to the levees. This was done by comparing the orientation and position of levee complexes relative to the channel belts or by tracing levee deposits in cross sections. Assigning ages to levees was hampered by diachronous activity within individual generations of channel belts. This concerns the pace in which levees expand in a cross-channel direction into the flood basin as well as vertical levee aggradation over time (see Appendices A2.2 and A2.3). Considering this we estimate that mature levee complexes in the period of interest can be dated with a precision of ± 200 years, which is slightly less than the precision at which the channel belt systems can be dated (± 100 years; Stouthamer and Berendsen, 2001). This makes the 400-year interval between the 100, 500, and 900 CE maps the most suitable time steps for levee planform comparison within the available data. For the palaeo-DEMs, additional assumptions on vertical levee aggradation had to be made. Considering the present state of geological dating control, the 100 and 900 CE elevation maps are considered to be the most optimal time steps. The accuracy of relative levee elevation reconstructions is estimated to be ± 17 cm based on errors in individual lithological borehole descriptions and in the groundwater level reconstructions used as the reference surface (see Appendix A2.3). The age and surface expression are more uncertain for older natural levees positioned deeper in the substrate and for stacked levees that occur in areas where the channel-belt density is high (such as in the upstream and central delta segments). The relative elevations resulting from our reconstructions were compared to those of archaeological settlements known to be positioned on the higher parts of the levee landscape (Roorda and Wiemer, 1992; Wiemer, 2002, updated in Van Lanen and Pierik, 2017). The settlement finds are most abundant above or around the reconstructed groundwater level (Appendix B), supporting the suitability of the reference surface in expressing levee height as relative elevation. Although the reconstructions proved to be valuable on a delta scale and for comparing individual channel belts, it cannot always be fully assessed at this stage as to what extent variation in local height (within smaller parts of individual alluvial ridges) represents real relief undulation or error noise. Nevertheless, we can comfortably state that levee dimensions show considerable variation on the scale of individual channel belts. This confirms the conclusion of Törnqvist and Bridge (2002) that many levees do not show idealized dimensions (e.g., widths or slopes), which are easily quantified and which would serve as a critical threshold for predicting avulsion. The pacing of lateral-levee development as well as distinguishing between initial stage crevasse splays and mature channel-belt levees could be further refined by detailed local sedimentological and geoarchaeological research focussed on the stratigraphy of single channel-belt generations. This could also help to better distinguish multiple generations of stacked levees and to include their dimensions in the already found delta-wide trends.

Identifying and isolating the roles of different levee-forming processes and their controls from the reconstructed palaeo-landscape maps remains a challenge. Process-based modelling (e.g., Nicholas et al., 2006) might be used as a complementary approach to test the relative importance of controls on levee evolution, such as the role of valley width, flood basin configuration, or riparian vegetation. Vice versa, the presented reconstructions can serve as validation for those modelling studies for scenarios with comparable initial and boundary conditions. Besides using numerical models, the mechanisms and controls proposed in the present study could be further tested by performing more detailed sedimentological research on selected isolated channel belts that were predominantly influenced by single controls. For such work, the maps of this study provide a way to select such test locations, where presumed controls are best expressed in levee shape. Sedimentological analysis on targeted channel belts could improve quantification of the development of levee growth through time and could help unravel the relative roles of levee-forming controls. Examples of paired selections of channel belts to isolate the effect of the controls are the varying distribution of discharge over bifurcating channels (levees of the Nederrijn vs. Waal channel belts; Fig. 7), the effect of downstream decreasing delta plain slope (levees of the Homoet/Kamp vs. Hennisdijk vs. Alm/Werken channel belts; Fig. 9A, C, D), or increased sediment load (levees of the pre-100 CE Herveld vs. 900 CE Nederrijn channel belts; in Fig. 8B). Combining delta-wide geomorphological studies with results from selected case studies and process-based modelling studies will

further enhance the understanding on levee development as important components in fluvial geomorphology.

5.3. Further applications

The advanced mapping of natural levees as executed in this study is only possible in deltaic and coastal areas for which large amounts of data have been collected and integrated. Because geomorphological and lithological data are generally most abundant for the shallow parts of a delta, mapping works best for relatively young deposits. The mapping could be extended to older deposits (formed in the first millennium BCE or earlier), but because data density is lower for these deposits (owing to erosion or burial by younger elements) the method will only yield comparable quality as the current study for smaller, well-preserved and well-explored areas (e.g., as done by Arnoldussen, 2008).

With our palaeo-DEMs, it is now possible to systematically distinguish between lower and higher parts of the levee landscape (i.e., within alluvial ridges of single channel-belt generations) — for the first time at delta scale. The levee reconstructions of our study therefore provide a starting point for archaeological prediction maps (e.g., Cohen et al., 2017a, 2017b) and modelling studies that focus on human-landscape interactions in the delta (e.g., Van Lanen et al., 2015a, 2015b; Groenhuijzen and Verhagen, 2016). The maps also provide a landscape zonation template for vegetation reconstructions (Peeters, 2007; Brouwer Burg, 2013; Van Beek et al., 2015), which in turn may be used to further enhance hydraulic modelling scenarios of delta flood dispersal (e.g., Van Oorschot et al., 2015). Including vegetation-morphology interactions would be an important step to test the hypotheses on variable levee morphology generated in this study.

6. Conclusions

In this paper we explored the controls on natural levee formation in the Rhine-Meuse delta. The detailed delta-wide reconstructions of natural levee surface elevation for the first millennium CE revealed levee patterns from which the following conclusions can be drawn:

- Our results strongly suggest that delta-scale natural preconditions (delta plain confinement, flood basin configurations, and substrate) were important controls in levee shape. Levee dimensions are not solely determined by channel dynamics but also by the hydraulic conditions in the inundated flood basins. This is demonstrated for the upper delta where delta plain confinement (from > 20 to 10 km wide) and the presence of older alluvial ridges amplified flood levels that generated higher natural levees (1–2 m above distal flood basin groundwater levels). The importance of flood basin hydraulics is confirmed by the strong tendency for wider levees in the direction of the decreasing flood basin slope along N-S oriented channel belts, suggesting that flood basin slope affected levee-forming hydraulics. Examples of the influence of the substrate were found in the downstream delta. Here, presence of peat close to the channel and under the levees led to levee subsidence and channel fixation, resulting in narrow but rather thick levees.
- Natural levees in the central to lower delta parts show a considerable decrease in width. This can be explained by a downstream depletion of suspended load caused by efficient sediment trapping of coarse-grained overbank sediment. This was facilitated by hampered flow and sediment-rich water trapping in the upstream enclosed flood basins. Most likely, the effect was further aided by differences in riparian vegetation density: in the deforested upstream part, the smaller lateral reduction in flow velocity allowed conveyance of overbank material farther away from the channel, leading to wider levees.
- Avulsions in the first millennium CE led to the formation of new levee complexes along the newly formed river channels over a considerable area in the former flood basins. The new river courses avoided the higher elevated areas with abundant fossil alluvial ridges in the landscape. On these fossil ridges, topographic levelling occurred resulting from widespread flood basin trapping of overbank sediment. Increased flooding frequencies combined with large suspended sediment loads during the first millennium CE caused the newly formed local levee crest heights to be 0.5 to 1.0 m higher than their predecessors. These higher levees possibly increased the chance for avulsion by enhancing cross-channel slope and enlarged meander wavelength because higher levees increased bankfull discharge.

Our new GIS-based reconstruction maps of the natural levee landscape serve as a starting point for more detailed sedimentological research and as field evidence for process-based numeric modelling studies. They additionally facilitate new opportunities for compiling palaeoenvironmental and geoarchaeological maps to further study the interaction between the past geomorphological processes, vegetation, and habitation.

Acknowledgements

This paper is part of the project ‘The Dark Ages in an interdisciplinary light’ funded by NWO (project nr. 360-60-110). The authors thank Bart Makaske (Wageningen University) for the first version of the new geomorphological map of the river area and Marieke van Dinter (Utrecht University/ADC) for the palaeogeographical map of the area around Utrecht. This paper benefited from discussions with Marjolein Gouw-Bouman, Marieke van Dinter (Utrecht University/ADC), and the participants of the workshop Dark Ages of the Lowlands 2015 listed on: http://darkagesproject.com/conferences. We would like to thank Hans Middelkoop, Bart Makaske, and three anonymous reviewers for their useful comments on the manuscript.

Appendix. Supplementary data

Supplementary data to this article can be found online at http://dx.doi.org/10.1016/j.geomorph.2017.07.003.

References

Adams, P.N., Slingerland, R.L., Smith, N.D., 2004. Variations in natural levee morphology in anastomosed channel flood plain complexes. Geomorphology 61, 127–142. http://dx.doi.org/10.1016/j.geomorph.2003.10.005.

Allen, J.R.L., 1965. A review of the origin and characteristics of recent alluvial sediments. Sedimentology 5, 89–191.

Arnoldussen, S., 2008. A Living Landscape: Bronze Age Settlement Sites in the Dutch River Area (c. 2000–800 BC). Sidestone Press, Leiden (535 pp).

Aslan, A., Autin, W.J., Blum, M.D., 2005. Causes of river avulsion: insights from the late Holocene avulsion history of the Mississippi River, U.S.A. J. Sediment. Res. 75, 650–664. http://dx.doi.org/10.2110/jsr.2005.053.

Berendsen, H.J.A., 1982. De genese van het landschap in het zuiden van de provincie Utrecht. Utrecht University, Utrecht.

Berendsen, H.J.A., 2007. History of Geological Mapping of the Holocene Rhine-Meuse Delta, The Netherlands. pp. 165–177.

Berendsen, H.J.A., Stouthamer, E., 2000. Late Weichselian and Holocene palaeogeography of the Rhine–Meuse delta, The Netherlands. Palaeogeogr. Palaeoclimatol. Palaeoecol. 161, 311–335. http://dx.doi.org/10.1016/S0031-0182(00)00073-0.

Berendsen, H.J.A., Stouthamer, E., 2001. Palaeogeographic development of the Rhine-Meuse delta, the Netherlands. Koninklijke van Gorcum, Assen (268p).

Berendsen, H.J.A., Volleberg, K.P., 2007. New Prospects in Geomorphological and Geological Mapping of the Rhine-Meuse Delta – Application of Detailed Digital Elevation Maps Based on Laser Altimetry.

Berendsen, H.J.A., Cohen, K.M., Stouthamer, E., 2007. The use of GIS in reconstructing the Holocene palaeogeography of the Rhine–Meuse delta, The Netherlands. Int. J. Geogr. Inf. Sci. 21, 589–602. http://dx.doi.org/10.1080/13658810601064918.

Bos, I.J., Stouthamer, E., 2011. Spatial and temporal distribution of sand-containing basin fills in the Holocene Rhine-Meuse Delta, the Netherlands. J. Geol. 119, 641–660. http://dx.doi.org/10.1086/661976.

Brierley, G.J., Ferguson, R.J., Woolfe, K.J., 1997. What is a fluvial levee? Sediment. Geol. 114, 1–9. http://dx.doi.org/10.1016/S0037-0738(97)00114-0.

Brouwer Burg, M., 2013. Reconstructing “total” paleo-landscapes for archaeological investigation: an example from the central Netherlands. J. Archaeol. Sci. 40,

2308–2320. http://dx.doi.org/10.1016/j.jas.2013.01.008.
Bryant, M., Falk, P., Paola, C., 1995. Experimental study of avulsion frequency and rate of deposition. Geology 23, 365–368. http://dx.doi.org/10.1130/0091-7613(1995)023<0365.
Cazanacli, D., Smith, N.D., 1998. A study of morphology and texture of natural levees-Cumberland Marshes, Saskatchewan, Canada. Geomorphology 25, 43–55. http://dx.doi.org/10.1016/S0169-555X(98)00032-4.
Cohen, K.M., 2003. Differential Subsidence within a Coastal Prism - Late-Glacial - Holocene Tectonics in the Rhine-Meuse Delta, the Netherlands. Ph.D. Dissertation Univ. Utrecht.
Cohen, K.M., 2005. 3D geostatistical interpolation and geological interpretation of paleo-groundwater rise in the Holocene coastal prism in the Netherlands. In: River Deltas - Concepts, Models and Examples. SEMP, pp. 341–364.
Cohen, K.M., Gouw, M.J.P., Holten, J.P., 2005. Fluvio-deltaic flood basin deposits recording differential subsidence within a coastal prism (central Rhine – Meuse delta, The Netherlands). In: Special Publications IAS 35pp. 295–320.
Cohen, K.M., Stouthamer, E., Hoek, W.Z., Berendsen, H.J.A., Kempen, H.F.J., 2009. Zand in banen - zanddieptekaarten van het Rivierengebied en het IJsseldal in de provincies Gelderland en Overijssel.
Cohen, K.M., Stouthamer, E., Pierik, H.J., Geurts, A.H., 2012. Digital Basisbestand Paleogeografie van de Rijn-Maas Delta/Rhine-Meuse Delta Studies' Digital Basemap for Delta Evolution and Palaeogeography. http://dx.doi.org/10.17026/dans-x7g-sjtw.
Cohen, K.M., Arnoldussen, S., Erkens, G., van Popta, Y.T., Taal, L.J., 2014. Archeologische verwachtingskaart uiterwaarden rivierengebied. In: Deltares Raport 1207078.
Cohen, K.M., Toonen, W.H.J., Weerts, H.J.T., 2016. Overstromingen van de Rijn gedurende het Holoceen: relevantie van de grootste overstromingen voor archeologie van het Nederlandse rivierengebied. In: Deltares Report, (Utrecht).
Cohen, K.M., De Bruijn, R., Marges, V., De Vries, S., Pierik, H.J., Vos, P.C., Erkens, G., Hijma, M.P., 2017a. Production of buried-landscape maps for Holocene-covered Netherlands, Map layer T0123 for the RCE Kenniskaart portal. In: Deltares Report 1210450-0013, (Utrecht).
Cohen, K.M., Dambrink, R., De Bruijn, R., Marges, V.C., Erkens, G., Pierik, H.J., Koster, K., Stafleu, J., Schokker, J., Hijma, M.P., 2017b. Mapping buried Holocene landscapes: past lowland environments, palaeoDEMs and preservation in GIS. In: Lauwerier, R.C.G.M., Eerden, M.C., Groenewoudt, B.J., Lascaris, M.A., Rensink, E., Smit, B.I., Speleers, B.P., Van Doesburg, J. (Eds.), Knowledge for Informed Choices: Tools for More Effective and Efficient Selection of Valuable Archaeology in The Netherlands. Ned. Archeol. Rapp. Vol. 55. Cultural Heritage Agency, Amersfoort, pp. 73–93.
Corenblit, D., Tabacchi, E., Steiger, J., Gurnell, A.M., 2007. Reciprocal interactions and adjustments between fluvial landforms and vegetation dynamics in river corridors: a review of complementary approaches. Earth-Sci. Rev. 84, 56–86. http://dx.doi.org/10.1016/j.earscirev.2007.05.004.
De Bakker, H., Schelling, J., 1989. Systeem van bodemclassificatie voor Nederland. In: De hogere niveaus, 2e gewijzigde druk. Wageningen, PUDOC.
De Boer, A.G., Laan, W.N.H., Waldus, W., Van Zijverden, W.K., 2008. LIDARbased surface height measurements: applications in archaeology. In: Fischer, B., Dakouri, A. (Eds.), Beyond Illustration: 2d and 3d Digital Technologies as Tools for Discovery in Archaeology. British Arch. Rep. Int. Series Vol. 1805. pp. 69–77.
Edelman, C.H., Eringa, L., Hoeksema, K.J., Jantzen, J.J., Modderman, P.J.R., 1950. Een bodemkartering van de Bommelerwaard boven den Meidijk. (STIBOKA).
Egberts, H., 1950. De bodemgesteldheid van de Betuwe. Wageningen, STIBOKA (82p).
Erkens, G., Cohen, K.M., 2009. Quantification of intra-Holocene sedimentation in the Rhine-Meuse delta: a record of variable sediment delivery. In: Erkens, G. (Ed.), Sediment Dynamics in the Rhine Catchment. Univ. Utrecht, pp. 117–172 Ph.D. Dissertation.
Erkens, G., Hoffmann, T., Gerlach, R., Klostermann, J., 2011. Complex fluvial response to late Glacial and Holocene allogenic forcing in the lower Rhine Valley (Germany). Quat. Sci. Rev. 30 (5), 611–627. http://dx.doi.org/10.1016/j.quascirev.2010.11.019.
Erkens, G., Toonen, W.H.J., Cohen, K.M., Prins, M.A., 2013. Unravelling mixed sediment signals in the floodplains of the Rhine catchment using end member modelling of grain size distributions. In: ICFS Proceedings 2010, . http://dspace.library.uu.nl/handle/1874/281634.
Erkens, G., van der Meulen, M.J., Middelkoop, H., 2016. Double trouble: subsidence and CO_2 respiration due to 1,000 years of Dutch coastal peatlands cultivation. Hydrogeol. J. 24 (3), 551–568.
Farrell, K.M., 2001. Geomorphology, facies architecture, and high-resolution, non-marine sequence stratigraphy in avulsion deposits, Cumberland Marshes, Saskatchewan. Sediment. Geol. 139, 93–150. http://dx.doi.org/10.1016/S0037-0738(00)00150-0.
Filgueira-Rivera, M., Smith, N.D., Slingerland, R.L., 2007. Controls on natural lev??e development in the Columbia River, British Columbia, Canada. Sedimentology 54, 905–919. http://dx.doi.org/10.1111/j.1365-3091.2007.00865.x.
Fisk, H.N., 1947. Fine-Grained Alluvial Deposits and their Effects on Mississippi River Activity. Corps of Engineers, Vicksburg, MS.
Funabiki, A., Saito, Y., Phai, V.V., Nguyen, H., Haruyama, S., 2012. Natural levees and human settlement in the Song Hong (Red River) delta, northern Vietnam. The Holocene 22, 637–648. http://dx.doi.org/10.1177/0959683611430847.
Gouw, M.J.P., 2007. Alluvial architecture of fluvio-deltaic successions: a review with special reference to Holocene settings. Geol. en Mijnbouw/Netherlands J. Geosci. 86, 211–227.
Gouw, M.J.P., 2008. Alluvial architecture of the Holocene Rhine-Meuse delta (the Netherlands). Sedimentology 55, 1487–1516. http://dx.doi.org/10.1111/j.1365-3091.2008.00954.x.
Gouw, M.J.P., Erkens, G., 2007. Architecture of the Holocene Rhine-Meuse delta (the Netherlands) – a result of changing external controls. Geol. en Mijnbouw/Netherlands J. Geosci. 86, 23–54.
Groenhuijzen, M.R., Verhagen, P., 2016. Testing the robustness of local network metrics in research on archeological local transport networks. Front. Digit. Humanit. 3, 6.
Guccione, M.J., 2008. Impact of the alluvial style on the geoarcheology of stream valleys. Geomorphology 101 (1), 378–401.
Guiran, A.J., 1997. Geologische waarnemingen in het tracé van de Willemsspoortunnel en de bewoningsgeschiedenis van Rotterdam. In: Carmiggelt, A., Guiran, A.J., van Trierum, M.C. (Eds.), BOORbalans 3: Archeologisch onderzoek in het tracé van de Willemsspoortunnel te Rotterdam.
Havinga, A.J., 1969. A physiographic analysis of a part of the Betuwe, a Dutch river clay area. Mededelingen Landbouwhogeschool Wageningen 69, 3. http://library.wur.nl/WebQuery/wurpubs/fulltext/299799.
Havinga, A.J., Op't Hof, A., 1983. Physiography and Formation of the Holocene Floodplain Along the Lower Course of the Rhine in the Netherlands. Wageningen, Landbouwhogeschool Wageningen.
Heitmuller, F.T., Hudson, P.F., Kesel, R.H., 2017. Overbank sedimentation from the historic A.D. 2011 flood along the lower Mississippi River, USA. Geology 45, 107–110. http://dx.doi.org/10.1130/G38546.1.
Heller, P.L., Paola, C., 1996. Downstream changes in alluvial architecture: an exploration of controls on channel-stacking patterns. J. Sediment. Res. 66.
Hesselink, A.W., Weerts, H.J.T., Berendsen, H.J.A., 2003. Alluvial architecture of the human-influenced river Rhine, The Netherlands. Sediment. Geol. 161, 229–248. http://dx.doi.org/10.1016/S0037-0738(03)00116-7.
Hoek, W.Z., 1997. Late-glacial and early Holocene climatic events and chronology of vegetation development in the Netherlands. Veg. Hist. Archaeobot. 6, 197–213.
Hudson, P.F., 2004. Geomorphic context of the prehistoric Huastec floodplain environments: lower Pànuco basin, Mexico. J. Archaeol. Sci. 31, 653–668. http://dx.doi.org/10.1016/j.jas.2003.06.002.
Hudson, P.F., Heitmuller, F.T., 2003. Local- and watershed-scale controls on the spatial variability of natural levee deposits in a large fine-grained floodplain: lower Pànuco basin, Mexico. Geomorphology 56, 255–269. http://dx.doi.org/10.1016/S0169-555X(03)00155-7.
Hudson, P.F., Middelkoop, H., Stouthamer, E., 2008. Flood management along the lower Mississippi and Rhine rivers (The Netherlands) and the continuum of geomorphic adjustment. Geomorphology 101, 209–236. http://dx.doi.org/10.1016/j.geomorph.2008.07.001.
Jones, L.S., Schumm, S.A., 1999. Causes of avulsion: an overview. In: Smith, N.D., Rogers, J. (Eds.), Fluvial Sedimentology. VI. International Association of Sedimentologists, pp. 171–178.
Kiss, T., Oroszi, V.G., Sipos, G., Fiala, K., Benyhe, B., 2011. Accelerated overbank accumulation after nineteenth century river regulation works: a case study on the Maros River, Hungary. Geomorphology 135, 191–202. http://dx.doi.org/10.1016/j.geomorph.2011.08.017.
Klasz, G., Reckendorfer, W., Gabriel, H., Baumgartner, C., Schmalfuss, R., Gutknecht, D., 2014. Natural levee formation along a large and regulated river: the Danube in the National Park Donau-Auen, Austria. Geomorphology 215, 20–33. http://dx.doi.org/10.1016/j.geomorph.2013.12.023.
Kleinhans, M.G., Ferguson, R.I., Lane, S.N., Hardy, R.J., 2013. Splitting rivers at their seams: bifurcations and avulsion. Earth Surf. Process. Landf. 38, 47–61.
Kolb, C.R., 1963. Sediments forming the bed and banks of the lower Mississippi River and their effects on river migration. Sedimentology 2, 227–234.
Kooistra, L.I., Dinter, M. Van, Dütting, M.K., Rijn, P. Van, 2013. Could the local population of the lower Rhine delta supply the Roman army? Part 1: the archaeological and historical framework. JALC 4, 5–23.
Koster, K., Stafleu, J., Cohen, K.M., 2016. Generic 3D interpolation of Holocene base-level rise and provision of accommodation space, developed for the Netherlands coastal plain and infilled palaeovalleys. Basin Res. 1–23. http://dx.doi.org/10.1111/bre.12202.
Lecce, S.A., 1997. Spatial patterns of historical overbank sedimentation and floodplain evolution, Blue River, Wisconsin. Geomorphology 18, 265–277.
Leopold, L.B., Wolman, M.G., 1960. River meanders. Geol. Soc. Am. Bull. 71 (6), 769–793.
Lewin, J., Ashworth, P.J., 2014. The negative relief of large river floodplains. Earth-Sci. Rev. 129, 1–23. http://dx.doi.org/10.1016/j.earscirev.2013.10.014.
Magilligan, F.J., 1985. Historical floodplain sedimentation in the Galena River basin, Wisconsin and Illinois. Ann. Assoc. Am. Geogr. 75, 583–594. http://dx.doi.org/10.1111/j.1467-8306.1985.tb00095.x.
Makaske, B., Smith, D.G., Berendsen, H.J.A., 2002. Avulsions, channel evolution and floodplain sedimentation rates of the anastomosing upper Columbia River, British Columbia, Canada. Sedimentology 49, 1049–1071. http://dx.doi.org/10.1046/j.1365-3091.2002.00489.x.
Makaske, B., Berendsen, H.J.A., van Ree, M.H.M., 2007. Middle Holocene Avulsion-Belt deposits in the Central Rhine-Meuse Delta, The Netherlands. J. Sediment. Res. 77, 110–123. http://dx.doi.org/10.2110/jsr.2007.004.
Makaske, B., Maas, G.J., Van Smeerdijk, D.G., 2008. The age and origin of the Gelderse IJssel. Geol. en Mijnbouw/Netherlands J. Geosci. 87, 323–337.
Minderhoud, P.S.J., Cohen, K.M., Toonen, W.H.J., Erkens, G., Hoek, W.Z., 2016. Improving age-depth models of fluvio-lacustrine deposits using sedimentary proxies for accumulation rates. Quat. Geochronol. http://dx.doi.org/10.1016/j.quageo.2016.01.001.
Modderman, P.J.R., 1948. Oudheidkundige aspecten van de Bodemkartering. Boor Spade 209–212.
Mohrig, D., Heller, P.L., Paola, C., Lyons, W.J., 2000. Interpreting Avulsion Process From Ancient Alluvial Sequences: Guadalope-Matarranya System (Northern Spain) and Wasatch Formation (Western Colorado). 112(12). pp. 1787–1803. http://dx.doi.org/10.1130/0016-7606(2000)112<1787.
Nicholas, A.P., Walling, D.E., Sweet, R.J., Fang, X., 2006. New strategies for upscaling

high-resolution flow and overbank sedimentation models to quantify floodplain sediment storage at the catchment scale. J. Hydrol. 329, 577–594. http://dx.doi.org/10.1016/j.jhydrol.2006.03.010.
Peeters, J.H.M., 2007. Hoge Vaart A 27 in Context: Towards a Model of Mesolithic - Neolithic Land Use Dynamics as a Framework for Archaeological Heritage Management. Ph.D. Dissertation Univ. of Amsterdam.
Pierik, H.J., Van Lanen, R.J., 2017. Roman and early-medieval occupation patterns in a delta landscape: the link between settlement elevation and landscape dynamics. Quat. Int.. http://dx.doi.org/10.1016/j.quaint.2017.03.010. (in press).
Pierik, H.J., Cohen, K.M., Stouthamer, E., 2016. A new GIS approach for reconstructing and mapping dynamic Late Holocene coastal plain palaeogeography. Geomorphology 270, 55–70. http://dx.doi.org/10.1016/j.geomorph.2016.05.037.
Pons, L.J., 1953. Oevergronden als Middeleeuwse afzettingen en overslag gronden als dijk doorbraakafzettingen in het rivierkleigebied. Boor en Spade 7, 97–111.
Pons, L.J., 1957. De geologie, de bodemvorming en de waterstaatkundige ontwikkeling van het Land van Maas en Waal en een gedeelte van het Rijk van Nijmegen. (Wageningen).
Pons, L.J., 1992. Holocene peat formation in the lower parts of the Netherlands. In: Verhoeven, J.T.A. (Ed.), Fens and Bogs in the Netherlands: Vegetation, History, Nutrient Dynamics and Conservation. Kluwer, pp. 7–79.
Pons, L.J., Zonneveld, I.S., 1965. Soil Ripening and Soil Classification: Initial Soil Formation of Alluvial Deposits with a Classification of the Resulting Soils. Veenman, Wageningen.
Roorda, I.M., Wiemer, R., 1992. The ARCHIS Project: Towards a New National Archaeological Record in the Netherlands. In: Larsen, C. (Ed.), Sites and Monuments: National Archaeological Records. The National Museum of Denmark, Copenhagen, pp. 117–122.
Shen, Z., Törnqvist, T.E., Mauz, B., Chamberlain, E.L., Nijhuis, A.G., Sandoval, L., 2015. Episodic overbank deposition as a dominant mechanism of floodplain and delta-plain aggradation. Geology 43 (10), 875–878.
Simm, D.J., Walling, D.E., 1998. Lateral variability of overbank sedimentation on a Devon flood plain. Hydrol. Sci. J. 43, 715–732.
Slingerland, R., Smith, N.D., 1998. Necessary conditions for a meandering-river avulsion. Geology 26 (5), 435–438. http://dx.doi.org/10.1130/0091-7613(1998)026<0435.
Smith, N.D., Perez-Arlucea, M., 2008. Natural levee deposition during the 2005 flood of the Saskatchewan River. Geomorphology 101, 583–594. http://dx.doi.org/10.1016/j.geomorph.2008.02.009.
Smith, N.D., Cross, T.A., Dufficy, J.P., Clough, S.R., 1989. Anatomy of avulsion. Sedimentology 36, 1–23.
Smith, N.D., Pérez-Arlucea, M., Edmonds, D.A., Slingerland, R.L., 2009. Elevation adjustments of paired natural levees during flooding of the Saskatchewan River. Earth Surf. Process. Landf. 34 (8), 1060–1068.
Steenbeek, R., 1990. On the Balance Between Wet and Dry: Vegetation Horizon Development and Prehistoric Occupation: A Palaeoecological-Micromorpho - Logical Study in the Dutch River Area. Ph.D. Dissertation Vrije Universiteit Amsterdam.
Stouthamer, E., 2001. Sedimentary products of avulsions in the Holocene Rhine–Meuse Delta, The Netherlands. Sediment. Geol. 145, 73–92. http://dx.doi.org/10.1016/S0037-0738(01)00117-8.
Stouthamer, E., Berendsen, H.J.A., 2001. Avulsion frequency, avulsion duration, and Interavulsion period of Holocene channel belts in the Rhine-Meuse Delta, The Netherlands. J. Sediment. Res. 71, 589–598. http://dx.doi.org/10.1306/112100710589.
Stouthamer, E., Cohen, K.M., Gouw, M.J.P., 2011. Avulsion and its implications for fluvial-deltaic architecture: Insights from the Holocene Rhine-Meuse Delta. In: Davidson, S.K., Leleu, S., North, C.P. (Eds.), From River to Rock Record: The Preservation of Fluvial Sediments and Their Subsequent Interpretation. Society for Sedimentary Geology, Special Publication Vol. 97. pp. 215–231.
Teunissen, D., 1988. De bewoningsgeschiedenis van Nijmegen en omgeving, haar relatie tot de landschapsbouw en haar weerspiegeling in palynologische gegevens. Mededelingen van de afdeling Biogeologie van de Discipline Biologie van de Katholieke Universiteit van Nijmegen 15 (108 pp).
Teunissen, D., 1990. Palynologisch onderzoek in het oostelijk rivierengebied—een overzicht. Mededelingen van de afdeling Biogeologie van de Discipline Biologie van de Katholieke Universiteit van Nijmegen 16 (163 pp).
Thonon, I., Middelkoop, H., Van der Perk, M., 2007. The influence of floodplain morphology and river works on spatial patterns of overbank deposition. Netherlands J. Geosci. 86, 63–75.
Toonen, W.H.J., Kleinhans, M.G., Cohen, K.M., 2012. Sedimentary architecture of abandoned channel fills. Earth Surf. Process. Landforms 37, 459–472. http://dx.doi.org/10.1002/esp.3189.
Toonen, W.H.J., Donders, T.H., Van der Meulen, B., Cohen, K.M., Prins, M.A., 2013. A composite Holocene palaeoflood chronology of the Lower Rhine. In: Toonen, W.H.J. (Ed.), A Holocene Flood Record of the Lower Rhine. Univ. Utrecht, pp. 137–150 Ph.D. Dissertation.
Toonen, W.H.J., Van Asselen, S., Stouthamer, E., Smith, N.D., 2016. Depositional development of the Muskeg Lake crevasse splay in the Cumberland Marshes (Canada). Earth Surf. Process. Landforms 41, 117–129. http://dx.doi.org/10.1002/esp.3791.
Toonen, W.H.J., Foulds, S.A., Macklin, M.G., Lewin, J., 2017. Events, episodes, and phases: signal from noise in flood-sediment. Geology 45, 331–334. http://dx.doi.org/10.1130/G38540.1.
Törnqvist, T.E., 1990. Fluvial activity, human activity and vegetation (2300–600 yr BP) near a residual channel in the Tielerwaard (central Netherlands). Ber. van Rijksd. voor het Oudheidkd. Bodemonderz. 40, 223–241.
Törnqvist, T.E., 1993. Fluvial Sedimentary Geology and Chronology of the Holocene Rhine-Meuse delta, The Netherlands. Ph.D. Dissertation Univ. Utrecht.
Törnqvist, T.E., Bridge, J.S., 2002. Spatial variation of overbank aggradation rate and its influence on avulsion frequency. Sedimentology 49, 891–905. http://dx.doi.org/10.1046/j.1365-3091.2002.00478.x.
Törnqvist, T.E., Van Dijk, G.J., 1993. Optimizing sampling strategy for radiocarbon dating of Holocene fluvial systems in a vertically aggrading setting. Boreas 22, 129–145.
Van Asselen, S., 2011. The contribution of peat compaction to total basin subsidence: implications for the provision of accommodation space in organic-rich deltas. Basin Res. 23, 239–255. http://dx.doi.org/10.1111/j.1365-2117.2010.00482.x.
Van Asselen, S., Cohen, K.M., Stouthamer, E., 2017. The impact of avulsion on groundwater level and peat formation in delta floodbasins during the middle-Holocene transgression in the Rhine-Meuse delta, The Netherlands. The Holocene 95968361770222. http://dx.doi.org/10.1177/0959683617702224.
Van Beek, R., Gouw-Bouman, M.T.I.J., Bos, J.A.A., 2015. Mapping regional vegetation developments in Twente (The Netherlands) since the late Glacial and evaluating contemporary settlement patterns. Netherlands J. Geosci. 2014, 1–27. http://dx.doi.org/10.1017/njg.2014.40.
Van Dijk, G.J., Berendsen, H.J.A., Roeleveld, W., 1991. Holocene water level development in The Netherlands' river area; implications for sea-level reconstruction. Geol. Mijnb. 70, 311–326.
Van Dinter, M., 2013. The Roman limes in the Netherlands: how a delta landscape determined the location of the military structures. Geol. en Mijnbouw/Netherlands J. Geosci. 92, 11–32. http://dx.doi.org/10.1017/S0016774600000251.
Van Dinter, M., Van Zijverden, W.K., 2010. Settlement and land use on crevasse splay deposits; geoarchaeological research in the Rhine-Meuse Delta, the Netherlands. Geol. en Mijnbouw/Netherlands J. Geosci. 89, 21–34.
Van Dinter, M., Cohen, K.M., Middelkoop, H., Hoek, W.Z., Stouthamer, E., Jansma, E., 2017. Abandonment history of the Roman and Medieval lower Rhine river and its influence on human occupation. (Quat. Sci. Rev.).
Van Helvoort, P.J., 2003. Complex confining layers: a physical and geochemical characterization of heterogeneous unconsolidated fluvial deposits using a facies-based approach. Netherlands, Geogr. Stud. 321 Utrecht. (147p).
Van Lanen, R.J., Pierik, H.J., 2017. Calculating connectivity patterns in delta landscapes: modelling Roman and early-medieval route networks and their stability in dynamic lowlands. Quat. Int.. http://dx.doi.org/10.1016/j.quaint.2017.03.009. (in press).
Van Lanen, R.J., Kosian, M.C., Groenewoudt, B.J., Jansma, E., 2015a. Finding a way: modeling landscape prerequisites for roman and early-medieval routes in the Netherlands. Geoarchaeology 30, 200–222. http://dx.doi.org/10.1002/gea.21510.
Van Lanen, R.J., Kosian, M.C., Groenewoudt, B.J., Spek, T., Jansma, E., 2015b. Best travel options: modelling Roman and early-medieval routes in the Netherlands using a multi-proxy approach. J. Archaeol. Sci. Rep. 3, 144–159. http://dx.doi.org/10.1016/j.jasrep.2015.05.024.
Van Oorschot, M., Kleinhans, M., Geerling, G., Middelkoop, H., 2015. Distinct patterns of interaction between vegetation and morphodynamics. Earth Surf. Process. Landforms 41, 791–808. http://dx.doi.org/10.1002/esp.3864.
Verbraeck, A., 1970. Toelichtingen bij de geologische kaart van Nederland, 1: 50.000, Blad Gorinchem Oost (38O), Rijks Geologische Dienst, Haarlem.
Verbraeck, A., 1984. Toelichtingen bij de geologische kaart van Nederland, 1: 50.000, Blad Tiel West (39W) en blad Tiel Oost (39O), Rijks Geologische Dienst, Haarlem.
Weerts, H.J.T., 1996. Fluvial, aeolian and organic facies units in the Rhine-Meuse delta. In: Weerts, H.J.T. (Ed.), Complex Confining Layers - Architecture and Hydraulic Properties of Holocene and Late-Weichselian Deposits in the Fluvial Rhine-Meuse Delta, The Netherlands. Univ. Utrecht, pp. 15–56 Ph.D. Dissertation.
Weerts, H.J.T., Berendsen, H.J.A., 1995. Late Weichselian and Holocene fluvial palaeogeography of the southern Rhine-Meuse delta (the Netherlands). Geol. en Mijnb. 74, 199–212.
Wiemer, R., 2002. Standardisation: the key to archaeological data quality. In: García Sanjuan, L., Wheatley, D.W. (Eds.), Mapping the Future of the Past, Managing the Spatial Dimension of the European Archaeological Resource, pp. 103–108 Sevilla.
Willems, W.J.H., 1986. Romans and Batavians. A Regional Study in the Dutch Eastern River Area. Ph.D. Dissertation Univ. of Amsterdam.